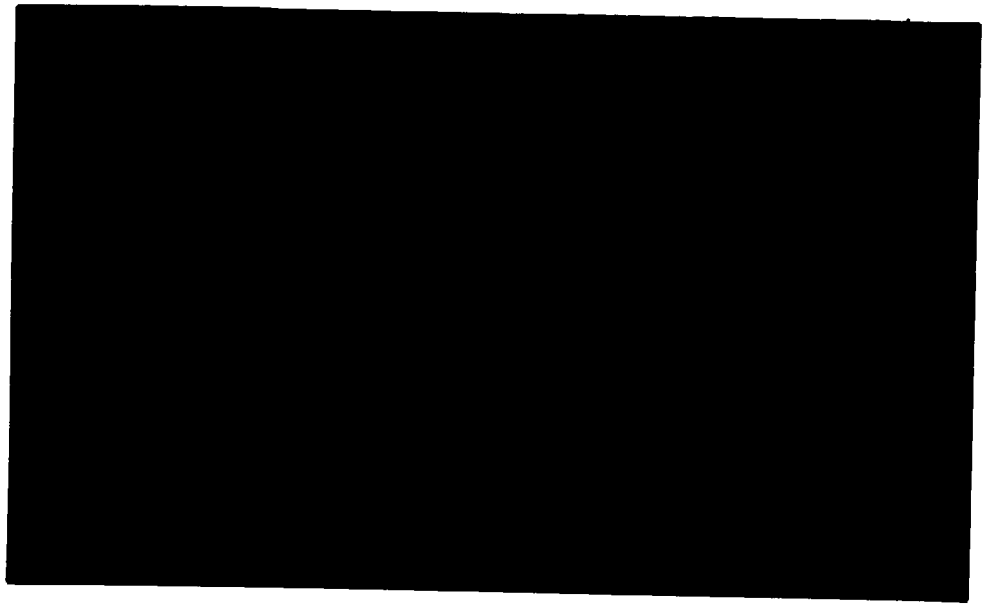

E
O
S

ELECTRO-OPTICAL SYSTEMS, INC.
A Subsidiary of Xerox Corporation
300 N. Halstead Street, Pasadena, California

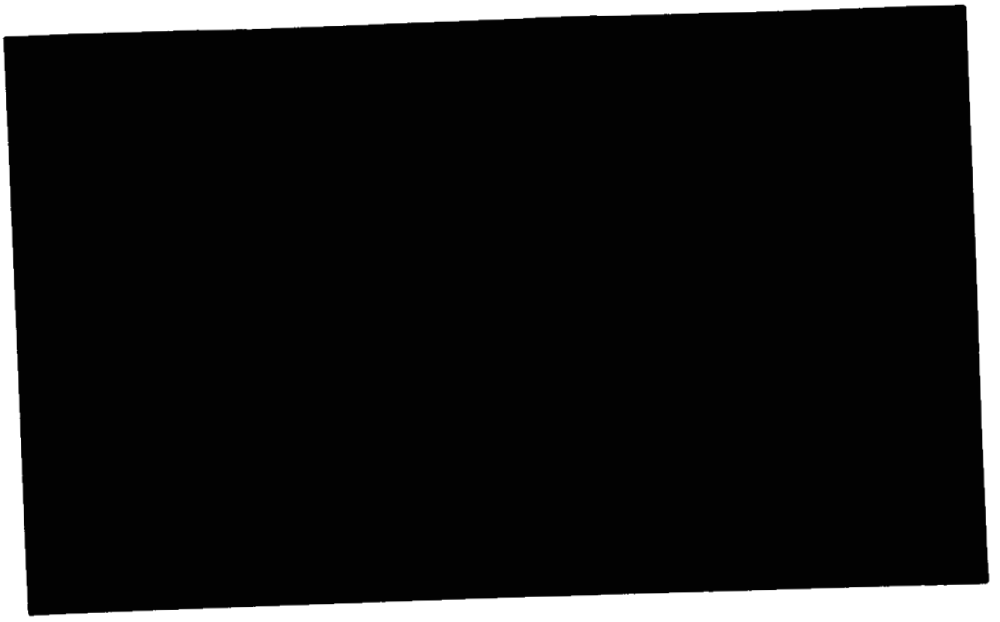

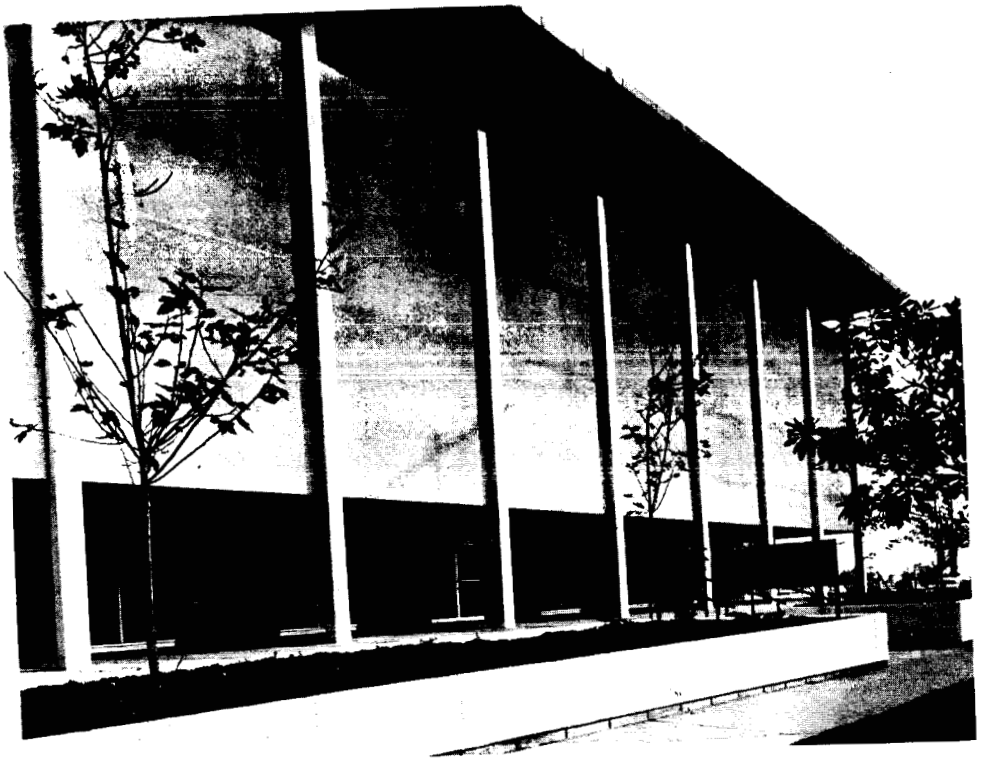

Fourth Monthly Report

SOLAR REFLECTING BEACON

Prepared for
National Aeronautics and Space Administration
Manned Spacecraft Center
Houston, Texas 77058

Contract NAS9-4790

EOS No. 6976-ML-4 26 October 1965

Prepared by
B. F. Kalensher
D. F. Stewart
OPTICS DIVISION

Approved by

C. W. Stephens, Manager

ELECTRO-OPTICAL SYSTEMS, INC. — PASADENA, CALIFORNIA
A Subsidiary of Xerox Corporation

CONTENTS

1. SUMMARY

This monthly report covers the period 17 September through 16 October 1965 and is submitted in accordance with the terms of contract NAS9-4790. The goal of this program is to develop conceptual and engineering designs for two types of Lunar Solar Reflecting Beacons emplaced during the early Apollo Lunar Landing Missions. One beacon will be visible from the earth. The other will be visible from both the Apollo Command Module and the Lunar Excursion Module vehicles. The scope of the program encompasses static and dynamic beacon design concepts including tracking beacons, photometric analysis of beacon detection, reliability as affected by the lunar environment, materials analysis, beacon location requirements, weight and packaging determinations, environmental and material specifications definition, engineering design of a recommended beacon and monthly, phase, and final reports.

The organization plan and the content of this monthly progress report conforms to the requirements of paragraph 3.2.1 titled Type I - Progress Reports, from NASA Interim Specification No. 25-1 dated 20 August 1964 and Article VIIA of the NAS9-4790 Contract Schedule.

Technical results for the fourth month of the program include:

1. Completed summary of equations, programs and computer data related to the orientation analysis including recommendations for possible future work in this area.
2. Calculations for terrestrial and cislunar beacon sizes as a function of visual and photographic observation.
3. Investigation of additional beacon concepts.
4. Analysis of orientation concepts.
5. Discussion of sun-pumped laser.

Management activities and work to be performed in the fifth month are described.

2. CONCLUSIONS AND RECOMMENDATIONS

The orientation analysis, exclusive of instrument location concepts, and the photometry calculations are complete. Beacon concept studies have accelerated in the past month.

A visit to MSC, NASA, Houston of 5 October clarified many program areas including alignment instruments, thermal-mechanical beacon concepts, and photographic mapping requirements. The program guidance and technical direction has been enhanced from this interchange.

Minimum recommended beacon sizes for various range and detector cases include:

a. Flat terrestrial beacon for both visual and photographic detection requires 1.53 square meters (2370 square inches).

b. Cislunar, 400-nautical-mile beacon, requires 1.03×10^{-4} square meters (0.155 square inches) or a sphere 4.95 meters in diameter (16.3 feet).

These areas were calculated assuming a lunar maria albedo of 0.065, a 0° phase angle, 99-percent detection probabilities for contrast, 1/2- and 2-second resolution for photographing and 1- and 5-second visual resolution angles from earth and cislunar locations, respectively. The area factors of safety for these beacons should probably range between 2 and 10. Since detailed experimental data and analysis on some recent Surveyor Landing Aids have not been published, the selection of safety factor values may be biased.

A sun-pumped laser offers promise as a beacon which could continuously transmit lunar experimental data.

The computer programs generated have particular value to the orientation of any communication device in space with respect to the earth or particular areas on the earth. Several of the beacon orientation and flash location computer subroutines could benefit

from greater simplification to produce more accurate answers in reduced running time using less memory space.

Several methods for orienting a fixed beacon are available, each of which requires celestial sightings and angular adjustments.

It is planned to present the beacon concepts in a matrix form in the phase I oral and written reports so that they may be more easily evaluated by classification and particular type as regards weight, packaging, area factor of safety, viewing time and frequency, reliability, erectability, etc. The explanation of classifications and types with several preliminary examples is given showing the general analysis for specific examples.

3. TECHNICAL RESULTS

3.1 Beacon Area Analysis

The area analysis presented in the last monthly report has been superseded and should be disregarded. The analysis detailed in Appendix A presents a much clearer interpretation of the subject and the various factors which influence the required beacon area. The reader will note the lack of any analysis of diffuse beacons. Weight and area penalties for diffuse beacons plus lower reflection values have so far favored the specular beacon concepts. These considerations will be presented in greater depth in later reports.

Table 3-I summarizes the minimum beacon areas calculated for photographic and visual observations from earth and cislunar orbit. Since the use of a 3.18 multiplication factor for the 50% probability of detection given by the Tiffany data may be questioned, the effect of increasing this factor to 10 and 100 on the required beacon areas, a_{10} and a_{100}, is shown together with the resultant factor of safety FS based on the calculated and minimum design area, a and a_d or a_{md} respectively, where

$$FS = \frac{a_d}{a}$$

Recommended design areas for the beacons, a_d, are also presented based on arbitrary safety factors of 2 for the earth-photographed beacon, 7.2 for the earth-visually-detected beacon (using 10 to 60-inch telescopes) and 11 and 10 for the cislunar photograph and visual beacons. These factors of safety will increase by almost a factor of 10 or correspondingly would allow greater resolution errors up to a factor of $\sqrt{10}$ as the phase angles approach $\pm 90^\circ$.

Beacon Area Analysis for Various Viewing Cases and Assumptions

Case	Contrast 1/ C_p or C_{50}	Minimum Design Area a_{md} m^2	Calculated Area a m^2	Factor of Safety a	2/ a_{10} m^2
1. Earth-photograph	0.08	1.53	1.53	1	--
2. Earth-visual	0.016	1.53	0.424	3.6	0.61
3. Cislunar-photograph	0.08	1.03×10^{-4}	0.91×10^{-5}	1.13	---
4. Cislunar-visual	0.0495	1.03×10^{-4}	1.03×10^{-4}	1	1.33×10^{-4}

See Text and Appendix A for Nomenclature.

1/ C_p = Photographic contrast

C_{50} = Tiffany 50% detection contrast

2/ a_{10} = area based on $10C_{50}$ visual contrast figure

3/ a_{100} = area based on $100C_{50}$ visual contrast figure

4/ FS d/a_{100} = design FS relative to a_{100} (instead of a)

TABLE 3-I

BEACON AREA CALCULATIONS

Factor of Safety a_{10}	a_{100} m^2 3/	Factor of Safety a_{100}	Recommended Design Area a_d m^2	Factor of Safety d	Factor of Safety d/a_{100} 4/	Range R nm	Resolution β sec
---	---	---	3.06	2	---	207,000	0.5
2.5	1.38	1.11	3.06	7.2	2.2	207,000	1.0
---	---	---	10×10^{-4}	11		400	2.0
0.77	5.03×10^{-4}	0.205	10×10^{-4}	10	2	400	5.0

Transmittance Telescope T_t	Transmittance Atmosphere T_e	Phase Angle Reflectance Factor K_θ	Beacon Reflectance r_b	Diametrical Magnification Factor M/D_o X/mm	Instrument Aperture Diameter D_o mm
0.7	0.7	1.0	0.80	---	280-1524
0.7	0.7	1.0	0.80	1.0	254-1524
0.7	1.0	1.0	0.80	---	>7.1
0.27	1.0	1.0	0.80	0.7	40.1

Even assuming that the Tiffany 50% values should be multiplied by 100, the design areas for visual detection have a factor of safety of 2 (i.e., twice the area required). The photographic beacon areas, assigned the same design values as the visual beacons, have a FS of 2 and 11 respectively for earth and cislunar detection.

The effect of good seeing requirements, particularly for terrestrial photography, is discussed in Appendix A.

Based on these large cislunar safety factors, omnidirectional spherical caps or lunes would require a spherical radius of 163 feet. This is impractical considering the tight weight tolerances. Therefore, since the beacon diameter varies as $\sqrt{a}$ or as R, consideration should be given to the reduction of the factor of safety or the range over which the beacon is visually sighted. A greater factor of safety seems to be essential for visual sightings, as opposed to photographic, since there are more uncertainties about the visual contrasts used. The tradeoffs between diameter, weight, and factors of safety will be discussed in conjunction with the beacon concepts.

Analysis of the beacon sizes cited above and in Table 3-I indicates that these new calculated areas are much larger than earlier area calculations found in the literature and depending on the FS and contrast values cited, the areas are equal to or less than some current predicted area requirements. The variations are in general due to

1. Lunar background assumptions
2. Limitations of resolution angle and the choice of resolution angle for computational purposes
3. Telescope magnification factor and its interrelationship with seeing conditions
4. Range
5. Telescope transmission
6. Choice of beacon reflectance

The effect of these is explained in Appendix A.

It becomes clear that rather than arbitrarily choosing a given value for each time-dependent variable, a probability function should be assigned. In this way an integrated probability of detection could be given as a figure of merit based on time-dependent variables such as:

1. Lunar background
2. Resolution angle
3. Telescope magnification
4. Atmospheric transmission
5. Beacon reflectance

Such an expression would be complex but would give a better concept of beacon reliability than arbitrarily chosen values.

3.2 Beacon Concepts

This section reflects the treatment which will be given all the beacon design concepts in the forthcoming Phase Report.

Beacon concepts can be classified into two broad categories and two major subheadings:

1. Omnidirectional
   - Static - continuous beacon
   - Dynamic - flashing beacon
2. Unidirectional
   - Static - flashing
   - Dynamic - flashing

General examples of these categories will be described along with a matrix basis of comparison and details of specific type.

3.2.1 General Concept Discussion

3.2.1.1 Omnidirectional Beacons

For the cislunar case, an omnidirectional beacon is a beacon which continuously shines or flashes in the 2π steradian or hemispherical portion of the celestial sphere bounded on the bottom by the local horizon at the beacon landing site. Such a beacon is either a hemisphere, spherical cap, or lune (a lune is the

surface between two meridians; i.e., the orange peel slice) or faceted approximation to a sphere where the area of each facet, a, is given by

$$a = \frac{\pi\alpha^2}{64} d_s^2$$

where α is the solar angular subtend and d_s the spherical diameter. Each facet will subtend a solid angle of

$$\frac{\pi\alpha^2}{16}$$

corresponding to an angular subtend of $\frac{\alpha}{2}$.

Since the flight plans of the CM and LEM vehicles are defined and since the selenographic latitude of the sun varies by less than ±2 degrees of arc, a complete hemispherical cap is not required. A complete lune ±47 degrees wide, and ±90 degrees long, located with its axis on the lunar landing site latitude and pointed with its plane of symmetry to the median solar selenographic latitude, will continuously reflect to 2- steradians and defines the maximum omnidirectional coverage required.

If the time of the mission is known, then a spherical cap ±45° in every direction with its optical axis pointed at the selenographic longitude and latitude of the sun at the time of the mission will be sufficient.

For earth viewing case, an "omnidirectional" beacon need only be a spherical arch ±4 degrees wide and ±45 degrees long to reflect solar rays continuously to the earth throughout each lunar month (i.e., ±1/2 the phase angle in length and ±1/2 the angular librations of the moon in width).

Since the range requirements for the cis-lunar beacon vary with the position of the CM and LEM vehicles in a ±5° latitude corridor, the area of a faceted spherical approximation can be decreased if the mission constraints on lunar phase angle are more closely defined.

An omnidirectional flashing beacon will rotate or oscillate so that a flash will be seen at any point within a 2π steradian field of view within a given time-span. The elapsed time and frequency of each flash will depend on the motion and area of the beacon.

Basic subheadings for omnidirectional beacons include:

STATIC

Spherical

1. Sphere - in balloon
2. Hemisphere
3. Lune
4. Cap - lenticular inflated reflector
5. Arch
6. Combinations of the above

Faceted

1. Hemispherical approximation
2. Lune - approximation
3. Cap - approximation; i.e., a flat in the limit
4. Arch
5. Combination of the above shapes

Miscellaneous - i.e., umbrella

DYNAMIC

Spherical

1. Lune
2. Cap
3. Cylinder
4. Arch
5. Combinations of the above

Faceted

1. Hemispherical approximation - geodesic dome
2. Lune approximation
3. Cap approximation - i.e., one flat in the limit
4. Cylinder approximation
5. Arch
6. Combinations of the above

Miscellaneous

3.2.1.2 Unidirectional Beacons

Unidirectional beacons are herein defined as flashing beacons which flash to only a portion of the 2π steradian field of view of the cislunar beacon or the solid angle defined by ±90 degrees selenographic longitude and ±8 degrees latitude for the earth beacon.

Similarly, unidirectional beacons will have the same basic subheadings as the omnidirectional beacons with the exception of those with completely omnidirectional shapes such as the sphere, hemisphere and hemispherical approximations. These subheadings will be used in the matrix to classify specific beacon concepts.

The range constraints as a function of the mission altitude and ±5° latitude corridor are shown in Fig. 3-1 and 3-2 for two planes, one including and one perpendicular to the north-south meridian passing through a beacon located at 0° latitude. When these range and mission constraints are completely defined, beacon area requirements for specific beacon designs can be reduced.

3.2.2 Beacon Concept Analysis Matrix

Table 3-II shows an example of the Beacon Concept Analysis Matrix which will be used to evaluate various beacon design concepts. Note that the flashing beacon area safety factor is based on the fact that below flash times of 0.1 sec, the area x time is a constant.

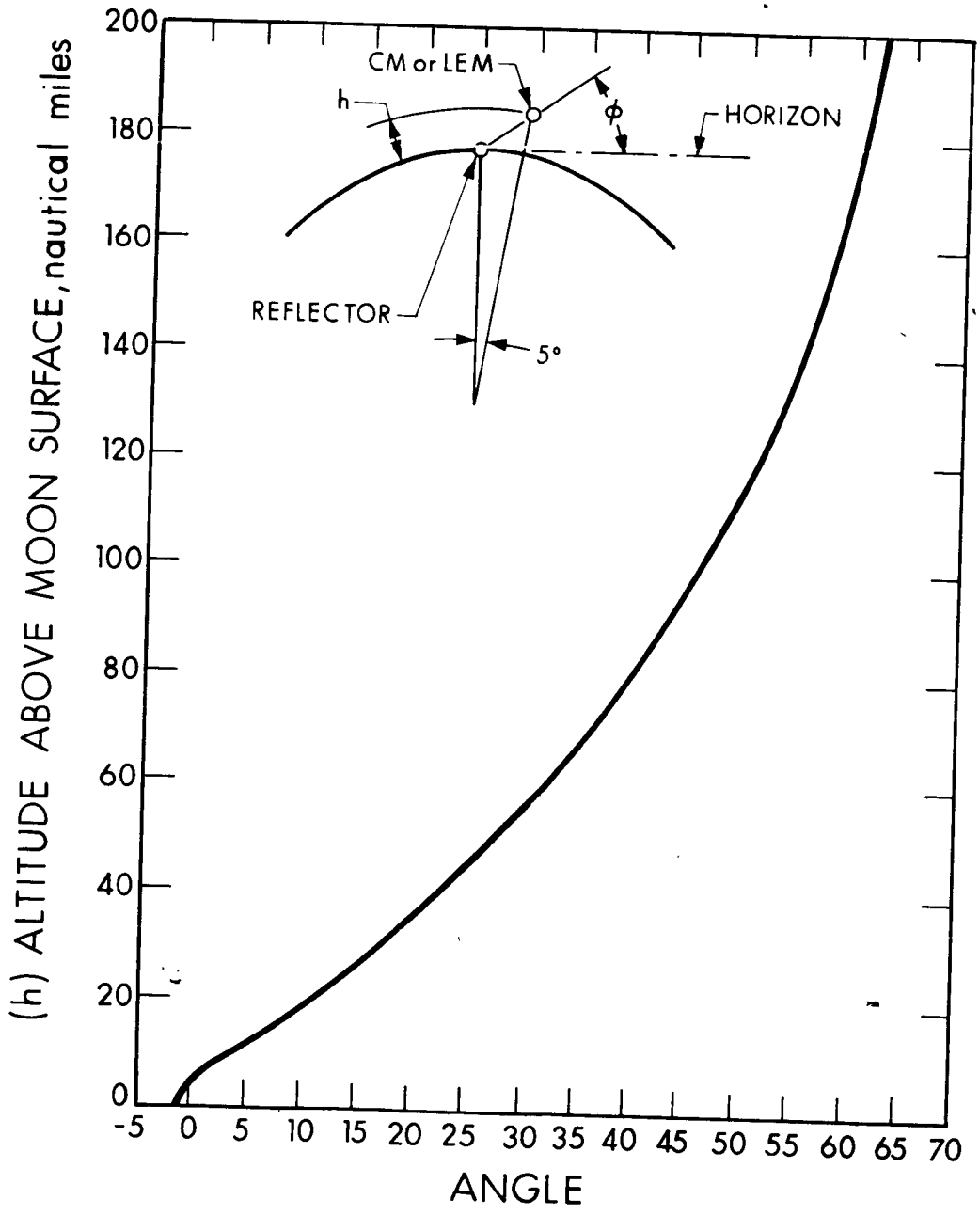

FIG. 3-1 ORBIT HEIGHT VS ELEVATION ANGLE FOR A 5° LATITUDE ORBIT IN THE PLANE DEFINED BY THE NORTH/SOUTH MERIDIAN THROUGH THE BEACON

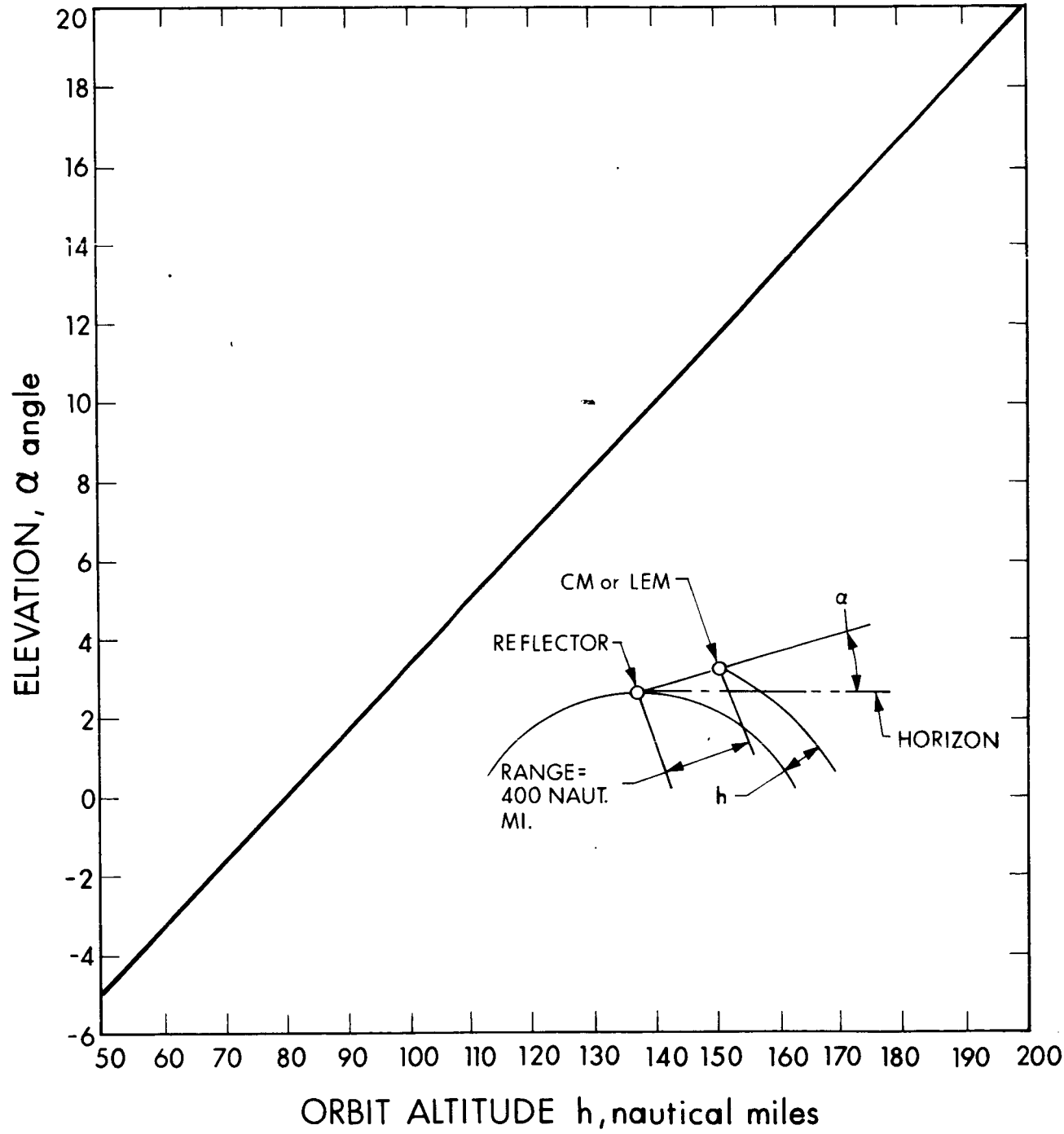

FIG. 3-2 ELEVATION ANGLE VS ORBIT ALTITUDE FOR A 400-NAUTICAL-MILE SLANT RANGE IN THE PLANE THROUGH THE LATITUDE OF THE BEACON

Classification Type	Figure	Weight Pounds	Volume Cu Ft	Area Ft^2 or in^2	FS (area) Visual	FS (area) Photo	Viewing Time t_v
Earth Beacons							
Omnidirectional							
Unidirectional							
1.2.3 One flat	3-3	10	1.0	3.06	7.2	2.0	20 min
Cislunar Beacons							
Omnidirectional							
1.1.4 Inflatable, rigidized cap	3-4	5	0.25	$\simeq$0.16 in^2	1	1.13	50%
2.1.2 Rotating paddles	3-5	4.0	0.25	1600 in^2	10*	11*	0.0001
2.1.3 Rotating Cylindrical segment	3-6	4.2	0.33	$\simeq$4.45 in^2	10*	11*	0.036

*FS based on an equivalent area based on the relationship $a_e = \frac{a_d t_v}{0.1}$

TABLE 3-II

PRELIMINARY BEACON CONCEPT ANALYSIS MATRIX

1/ Frequency	Reliability	Erectability Orientation Minutes	Advantages	Disad
yr	0.9	15	Meets weight, volume and FS requirements, metal mirrors	Alignment stability orientati Susceptib area, ere tion time
lunar month	0.5	2	Meets weight and volume requirements, short erection time; echo materials	Substand FS, susc meteorite
0.9 min	0.92	4	Meets weight, volume, reliability requirements, rotation minimizes dust settling	Time betw Electro-M Drive spd
0.9 min	0.95	6	Meets weight, reliability requirements, metal mirrors, lower dust susceptibility	Time betw over 2π s flash tim Drive, vo than desi

·antages	Comments	Rating
; dependent on / of lunar crust, .on accuracy.)le to dust; large :ction and orienta- : relatively long	Other related design concepts can reduce erection time.	
ard reliability and eptible to micro- : failure	Omnidirectional at one set of solar selenographic coordinates.	
veen flashes is long, Mechanical Drive, eds high	Drive speeds can be reduced by using faceted paddles; Thermal-Mechanical Drive under study.	
veen flashes, flashes teradians - wasting e, Electro-Mechanical lume slightly larger red	Frequency of flashes can be increased with small increase in cylinder weight - frequency proportional; Thermo-Mechanical Drive under study.	

Figures are shown depicting each beacon concept, Fig. 3-3, 3-4, 3-5, 3-6. Only on the rotating cylindrical segment beacon (Fig. 3-6) is the analysis given in detail. This is only representative of the matrix analysis approach and does not now represent our best recommendation for a cislunar beacon.

3.2.3 Rotating Cylindrical Segment Beacon Type 2.1.3

The cylindrical segment beacon, Fig. 3-6, is summarized in greater detail in Table 3-III. Basically the rotation of the cylinder approximates a complete hemisphere once every 54 seconds. The reflecting cylindrical segment panels are easily aligned and there are only a few assembly operations. However, the attachment of the panels to the supporting spokes may be difficult. No instrument orientation steps are required.

Electrical power for the rotor motor is supplied by 3 solar panels oriented to achieve uniform power levels throughout the solar day. Thermomechanical drives are now being studied.

Aside from the effects of micrometeorites and dust on the beacon itself, bearing, motor and solar panel and conversion panel life are major reliability considerations.

3.3 Sun-Pumped Laser

Appendix B describes the state of the art of a sun-pumped laser that has unique solar conversion and communication possibilities, which, combined with the attributes of the laser as a beacon, presents a novel approach to a solar-powered beacon. However, tracking and reliability considerations presently give it a low rating for this application.

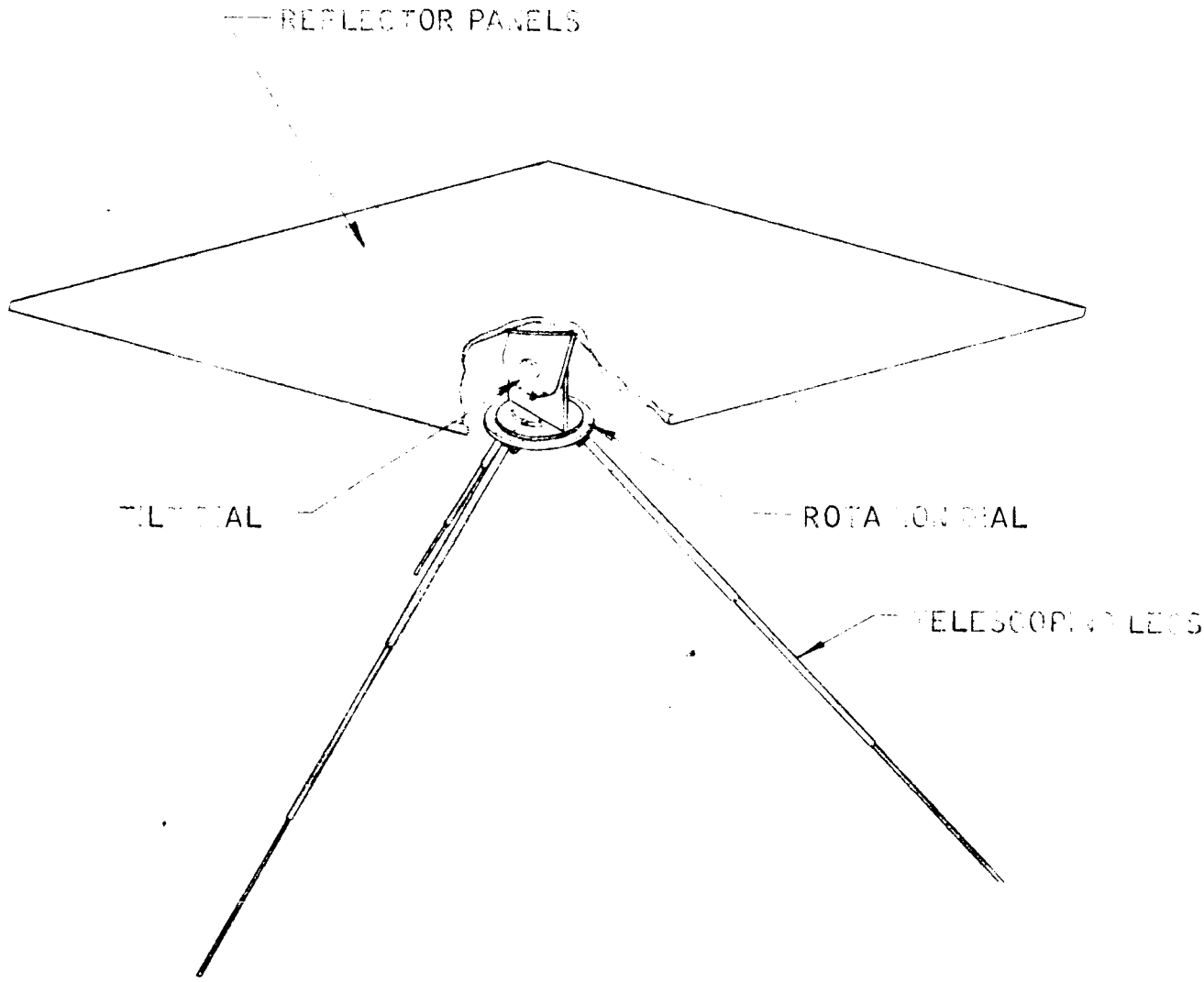

FIG. 3-3 FLAT EARTH BEACON

A - A

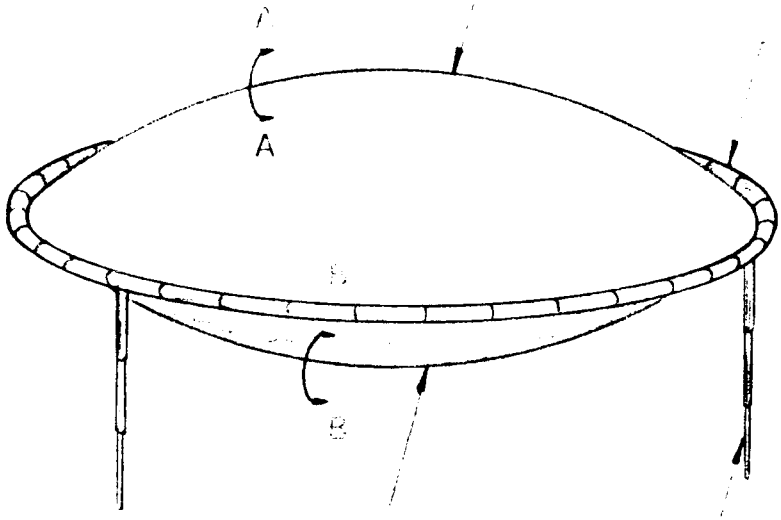

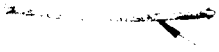

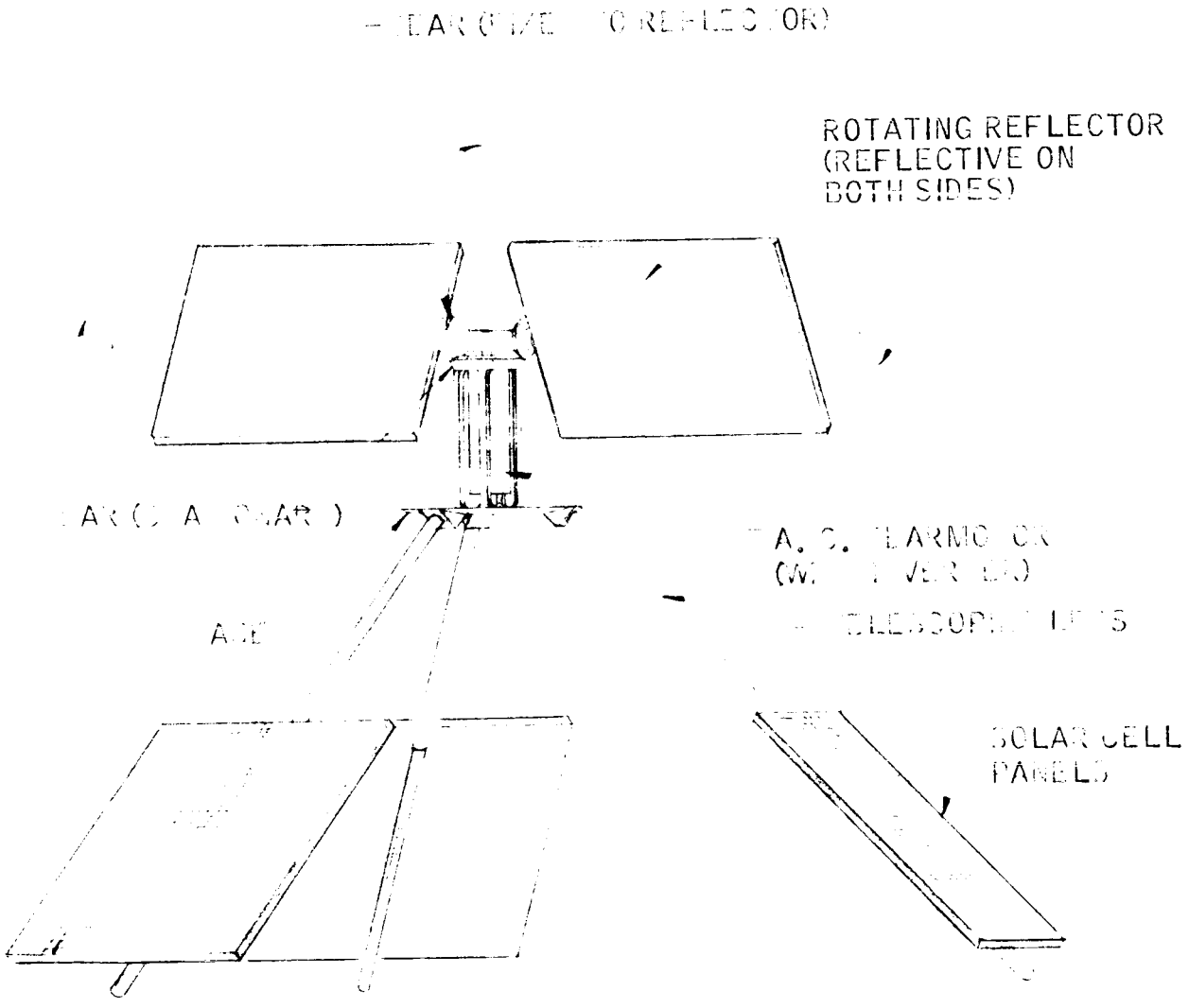
ROTATING REFLECTOR
(REFLECTIVE ON
BOTH SIDES)
A.C. ALTERNATOR
(WITH GEAR BOX)
SOLAR CELL
PANELS

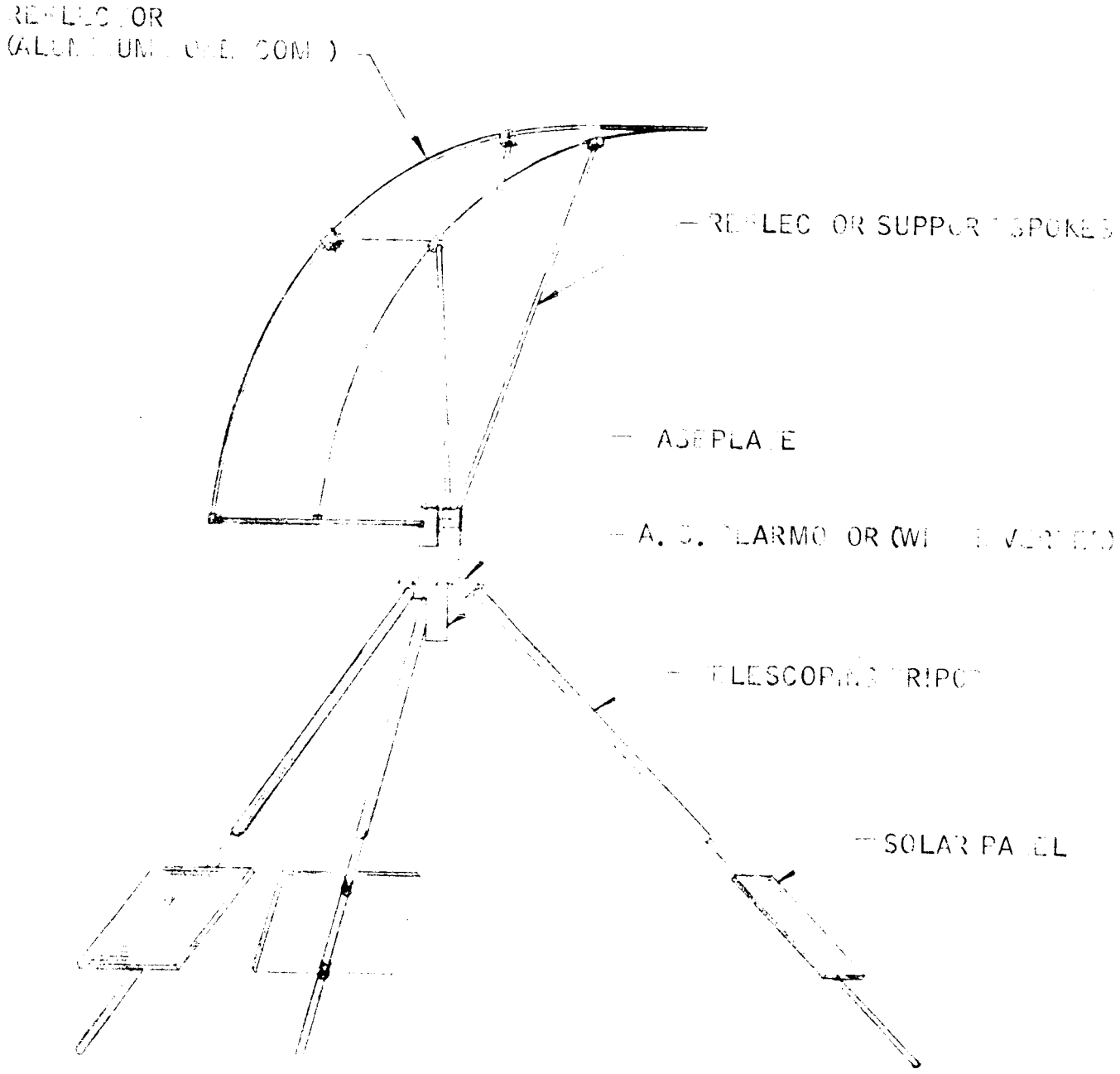

REFLECTOR CYLINDRICAL SECTION - EACH

TABLE 3-III

MATERIAL AND WEIGHT ANALYSIS - ROTATING CYLINDRICAL REFLECTOR

COMPONENT	MATERIAL	SIZE	WEIGHT OF COMPONENTS	COMMENTS
Gear-Motor	AC Induction Motor	1.07" dia × 2.8"	0.25 lb	Gaylord Rives
Inverter	Transistorized Construction	1⅜" × 1⅝" × 1¼"	0.20 lb	Gaylord Rives
Solar Cell Panels	Various Mat'l	6½" × 7¼" × 0.10 (3) Req'd	0.37 lb	For (3) Panels
Drive Train-Brgs., Shaft Assy. (w/Hub & Cross-arm), Hsg.	Brgs. - Teflon Shaft Assy. - Aluminum	---	0.05 lb	
Spokes	Aluminum	½" dia × 0.028 wall (6) Req'd	0.40 lb	
Reflector	Alum. Honeycomb	19" chord × 20" × 3"	1.00 lb	For 3 Segments
Support Ring & Hsg. Assy.	Aluminum	---	0.07 lb	
Tripod Legs	Aluminum	½ dia × 0.028 wall × 30" (3) Req'd	0.37 lb	For (3) Legs
Hardware (Screws, Lugs, Pins, etc.)	Aluminum	---	0.05 lb	
TOTAL (w/o Shipping Container)			2.76 lb	
Shipping Container		1/3 ft³	1.40 lb	Only ¼ ft³ Allowed
TOTAL WEIGHT (w/Shipping Container)			4.16 lb	

3.4 Ephemeris Tapes and Selenographic Coordinates

The information on the JPL ephemeris tapes has recently been transferred from the IBM fortran format to the CDC fortran format. This means that the rectangular position coordinates of the moon and earth ($\overline{X}_{em}$, Y_{em}, Z_{em} and $\overline{X}_{se}$, Y_{se}, Z_{se}, respectively) are now available and can be employed in Program I of the reflector orientation computer program to compute the earth-moon distance, R, the right ascension of the sun, α_s, and the selenographic coordinates of the earth and sun: μ_e, λ_e; μ_s, λ_s. These computations will be made within the next four weeks and the results given in the next monthly report.

Calculation of the earth's and sun's selenographic coordinates at one day intervals for the years 1965-1980 has finally been completed by JPL. They will give us this information on a single reel of magnetic tape. If we employ their results in our computer program, a large part of Program I can be eliminated. (Refer to Fig. 3-4 of the monthly report for September.)

3.5 Orientation of the Reflector by the Astronaut

The problem of determining the azimuth and elevation angles σ, γ of the reflector normal, relative to the moon's surface, which enable the reflected light to strike a given point on the earth's surface at a specified time, has already been solved. A preferred scheme for orienting the reflector in the desired direction γ, σ, however, has not yet been decided upon. Following, is a discussion of two basic methods for orienting the mirror.

3.5.1 Method (A)

In this method, the angles γ, σ are measured directly by the astronaut. In order to do so, he must be able to identify the direction from the mirror to the geometrical center of the moon, and the meridian passing through the reflector. If the former is determined by a plumb bob or a leveling device, the astronaut will establish the local vertical, and this could deviate from the desired reflector-moon center-direction by as much as $0^{\circ}.43$. (Refer to p. 11 of proposal to MSC.)

In order to locate the meridian (a great circle passing through the "north" and "south" poles of the moon) passing through the reflector, the astronaut must establish a reference plane which passes through the mirror-moon center direction and some specified point. This point could be a landmark on the moon with known latitude and longitude, or it could be a celestial body such as the sun, earth or a star. Having established this plane, the astronaut must then be able to identify the local meridian. Finally, he must orient the mirror in the desired direction γ, σ.

3.5.2 Method (B)

In this method, the astronaut does not measure γ, σ directly, but instead measures two other angles which automatically align the mirror normal along the desired γ, σ. A relatively simple example of this method is the location of the mirror normal-direction relative to the earth and the apparent earth-sun line, as seen from the reflector on the moon's surface. The two angles measured by the astronaut are then Ψ and β. A detailed description of these two angles, plus the theory underlying this orientation scheme, is given on pp. 14-15 of the third monthly report, September 24, 1965. The device employed by the astronaut to measure these angles is shown in Fig. 3-7. Here, the Reflector Pedestal is everything excluding the Sighting Mirror Assembly. The steps taken by the astronaut to align the reflector normal in the desired direction Ψ, β are as follows:

1. Attach Sighting Mirror Assembly to Reflector Platform (Eyepiece on SMA must be normal to Axis 1)
2. Set knob (a) (angle ζ) to 45 degrees and knob (b) (angle ξ) to 0 degree. Make sure that $\Psi = 0$ on Axis 1.
3. Rotate device on u-joint until earth is centered in eyepiece. Normal to Reflector Platform is now pointed at center of earth.
4. Rotate Reflector Platform through specified angle Ψ about Axis 1, and lock position.

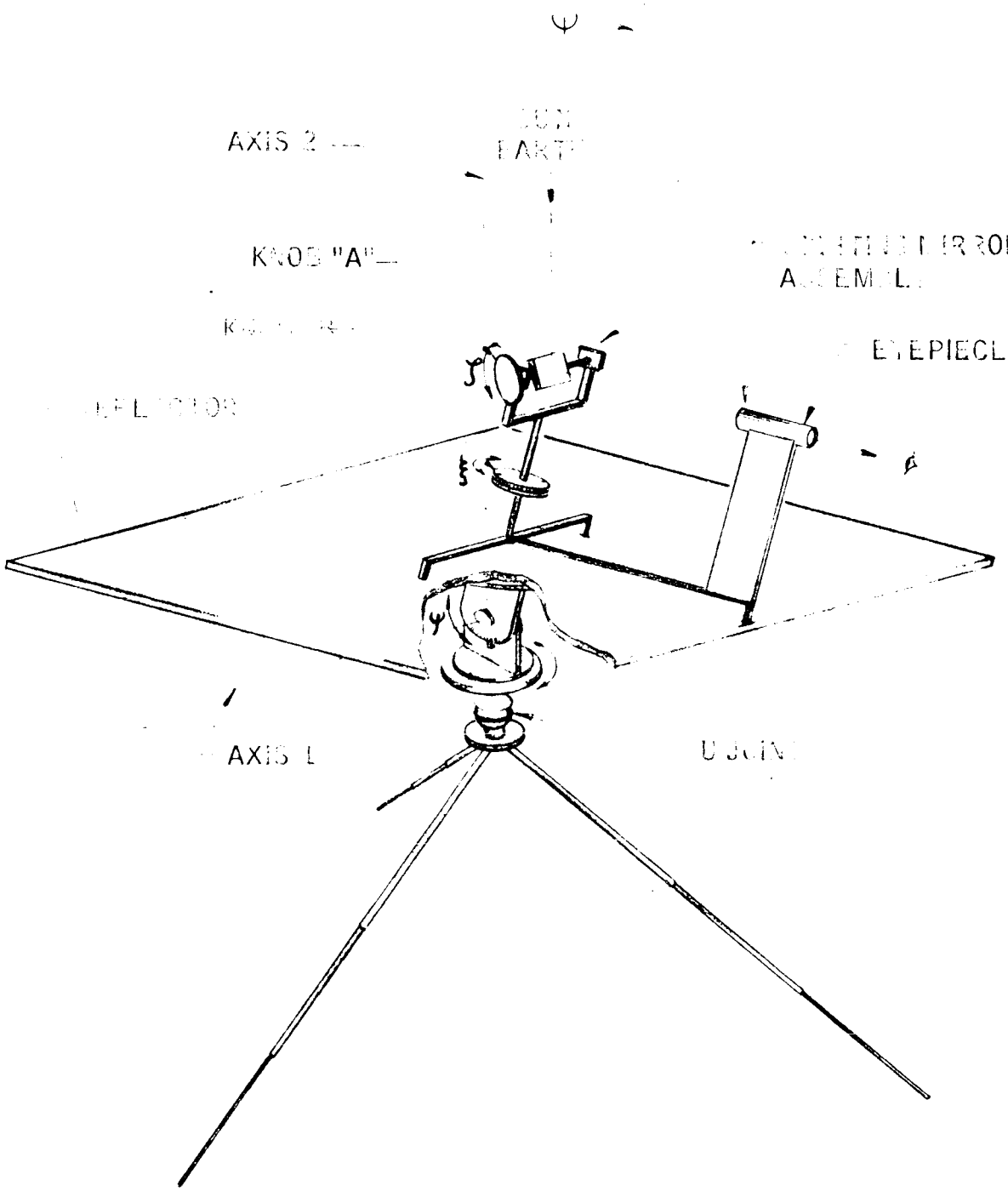

FIG. 3— REFLECTOR PEDESTAL PLUS SIGHTING MIRROR ASSEMBLY

5. Set knobs (a) and (b) to specified values of ζ and ξ, respectively. This aligns the normal of the sighting mirror in the proper direction to simulate β.
6. Rotate Reflector Platform about Axis 2 until sun is centered in eyepiece. Normal to Reflector Platform is now pointing in desired direction Ψ, β.
7. Remove the Sighting Mirror Assembly and attach reflector to platform.

Precomputed values of Ψ, ζ, ξ, at ten or twenty minute intervals, will be provided the astronaut, so that he may orient the Reflector Platform at his leisure. Expressions for ζ, ξ are given at the end of Appendix C.

The advantage of Method (B) over Method (A) is that the former avoids the necessity of establishing the local vertical and the local meridian. It will also be simpler for the astronaut to locate the earth and sun in the eyepiece than it will be to locate a specified star. Of course, errors will occur in the hand-adjustment of angles Ψ, ζ, ξ, but similar, or more serious, errors are likely to occur in the orientation scheme of Method (A).

The preferred orientation scheme should be decided upon after careful discussion.

3.6 Visibility of Reflected Light at Observation Station on Earth

As mentioned on pp. 15, 17 of the monthly report for September, the reflected light coming from the mirror on the moon's surface will be conical in shape (since the sun is not a point source of light) and will illuminate a circle on the earth's disc, with an average radius of 967 n. miles. Due to the axial rotation of the earth and the motion of the moon, the reflected light will move across the earth's surface. Of interest, then, are the times that an earth-bound observer enters and leaves the cone of light, or merely enters or leaves the light. The equations which determine the length of time that an observer on earth sees the reflected light have been programmed on the EOS digital

computer. They are given in the appendix. These equations constitute Program VII in Fig. 3-4, p. 19, of the September monthly report. An initial attempt to generate the visibility times on the digital computer gave inconclusive results, due to the use of $\cos H_1$, rather than $\sin H_1$ (refer to appendix). A new computation, employing the equations given in the appendix, will soon be made and the results will be published in next month's report.

4. PROGRAM MANAGEMENT

The manpower loading chart is shown in Fig. 4-1. Secretarial charges have not accumulated since publications have been doing the bulk of the typing. Since this program has minimal material and other direct charges, the financial position is directly proportional to the labor hours spent.

	Cumulative Hours Expended (Actual/Scheduled)				
Category	16 Jul	15 Aug	17 Sep	15 Oct	15 Nov
Engineer IV					
Kalensher	44/110	201/220	374/330	482/440	/550
Stewart	44/90	125/180	152/270	192/360	/450
Engineer I					
Starr	16/0	122/0	274/0	274/274	/274
Other Programmers	-	-	-	127/0	/450
Design Engineer					
Len Wolby	-	-	-	142/140	/260
Design Draftsman					
Thompson	0/50	45/120	47/190	47/190	/190
Secretary	0/30	0/60	0/90	0/120	/200
Publications	0/15	18.5/30	52/45	78.5/140	/200
Total	104/295	511.5/610	908/925	1343/1380	/1850

5. WORK TO BE PERFORMED DURING THE NEXT REPORTING MONTH

The following tasks will be performed during the next reporting month:

1. Complete beacon concepts including weight and packaging analysis
2. Complete orientation instrument details
3. Phase I report
4. Prepare Oral Presentation

   The following outline is tentatively planned for the 1 December Oral Presentation at NASA Houston:

Time	Subject	Speaker
9:00-9:10 a.m.	Introduction	Donald E. Stewart
9:10-9:20	Terminology	Dr. Bernard Kalensher
9:20-9:40	Photometry	D. Stewart
9:40-10:00	Materials and Environmental Resistance	D. Stewart
10:00-11:00	Design Concepts	D. Stewart
11:00-11:40	Orientation	Dr. Kalensher
11:40-12:00	Recommendations and Summary	D. Stewart
1:15- p.m.	General Discussion	Dr. Kalensher and D. Stewart

MASTER

DEVELOPMENT & PRODUCTION DEPART

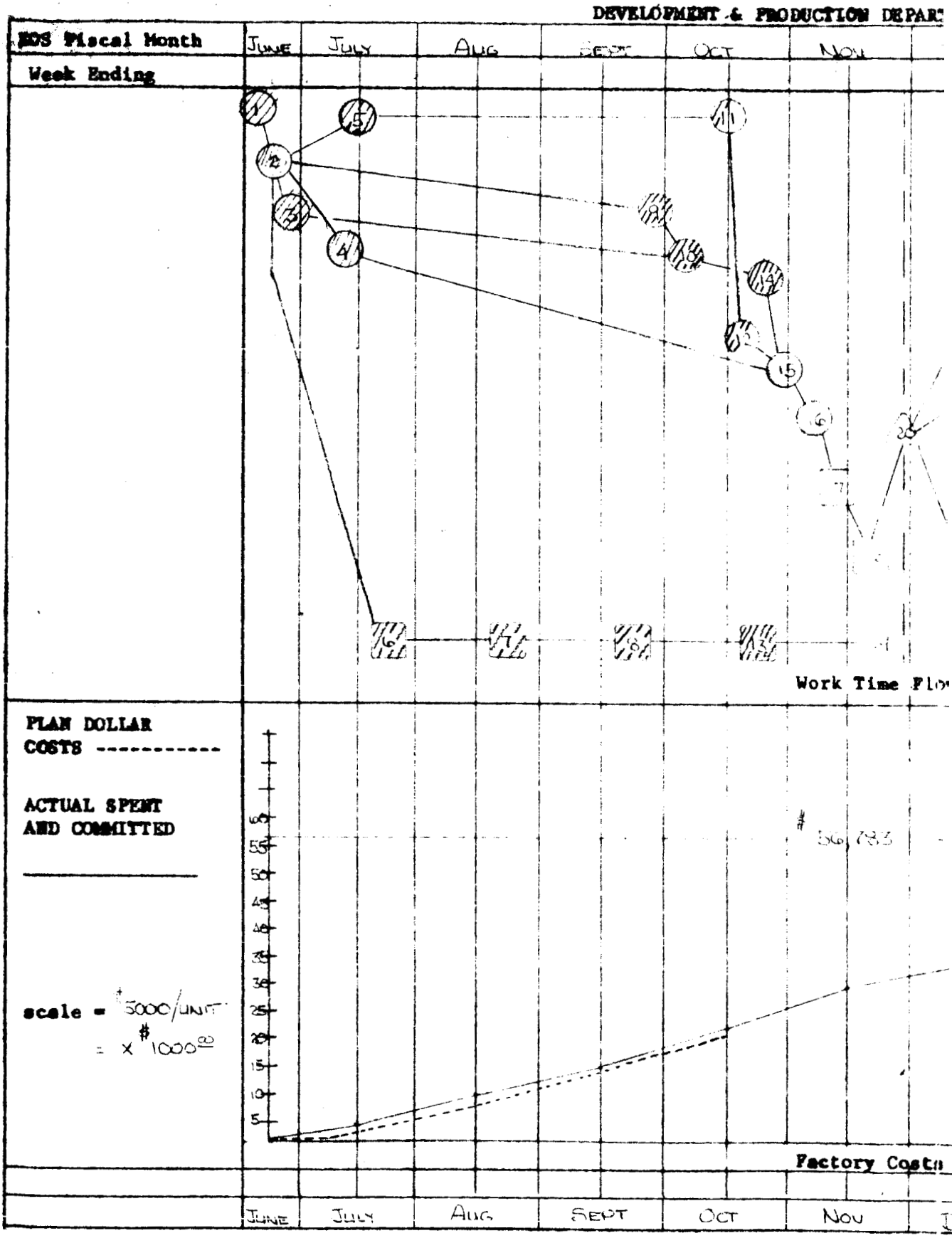

△ = Customer Milestone ○ = E.O.S. Milestone

PLAN

MENT - OPTICS DIVISION - E.O.S.

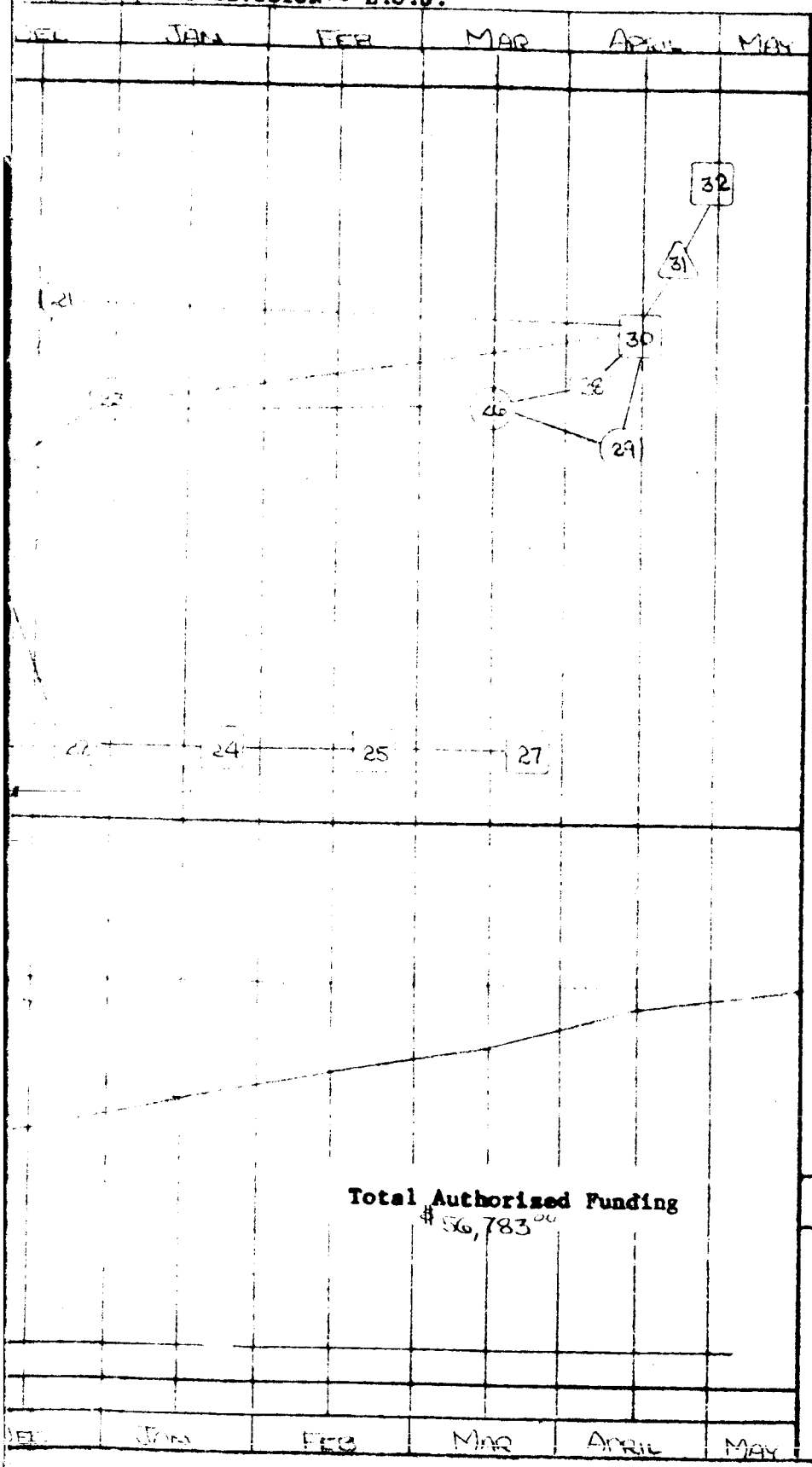

Total Authorized Funding
$56,783.00

Major Milestones

Milestone No.	Description
1.	CONTRACT AWARD
2.	EOS KICKOFF MEETING
3.	RECEIPT OF MISC DOCUMENTS
4.	TRACKING REQUIREMENTS
5.	LUNAR ENVIRONMENT SUMMARY
6.	MONTHLY #1
7.	MONTHLY #2
8.	MONTHLY #3
9.	PHOTO-OPTICAL ANALYSIS
10.	LOCATION ETC ANALYSIS - STATIC
11.	MATERIAL [illegible]
12.	[illegible] DESIGN CONCEPTS
13.	MONTHLY #4
14.	LOCATION ETC ANALYSIS - DYNAMIC
15.	DYNAMIC DEFINITION CONCEPTS
16.	PACKAGE AWT ANALYSIS
17.	PHASE I REPORT - WRITTEN
18.	PHASE I REPORT ORAL
19.	MONTHLY #5
20.	MSC APPROVAL
21.	ENVIRONMENTAL SPECIFICATIONS
22.	MONTHLY #6
23.	MATERIAL SPECIFICATIONS
24.	MONTHLY #7
25.	MONTHLY #8
26.	BEACON DESIGN
27.	MONTHLY #9
28.	WEIGHT & PACKAGING ANALYSIS
29.	BEACON TRAINING PACKAGE
30.	FINAL REPORT DRAFT
31.	FINAL REPORT APPROVAL
32.	FINAL REPORT DISTRIBUTION

Program: SOLAR REFLECTING BEACON

Survey Date: 7/16/65

Proj. Supervisor: D STEWART

Contract No.

Customer: MSC NASA, HOUSTON

EOS UA No. 6976-01,02,03-00

= E.O.S. Delivery

APPENDIX A

BEACON PHOTOMETRIC ANALYSIS

1. DETECTION VARIABLES

The reflective area required for the detection of lunar beacons depends upon the following variables:

1. Background brightness, B_f
2. Beacon reflectance, r_b
3. Sun-moon-instrument phase angle, θ
4. Instrument beacon range, R
5. Integrated instrument optical transmittance, T_t
6. Integrated instrument angular resolution as a function of aperture, instrument errors, atmospheric seeing (and for photographic records of the detector errors), β
7. Atmospheric transmittance, T_e
8. Contrasts required for a given detector and probability of detection, C_v - visual, C_p - photographic
9. Lunar beacon location

The following sections describe the analysis required for beacon sizing, the major variables in detail, representative calculations, and beacon area recommendations.

2. CAMERA PHOTOMETRY THEORY

With a camera, the field brightness, B_f, is decreased only by the atmospheric and camera transmittance losses, T_e and T_t, so that the apparent field brightness, B_{af}, at the detector is

$$B_{af} = T_e T_t B_f \qquad (1)$$

But B_f is related to the lunar field albedo or reflectance at 0° phase angle, a_f, the phase angle reflection ratio for a given lunar location, K_θ, the solar illuminance of the moon, E_s, and π so that

$$B_f = \frac{K_\theta \, a_f \, E_s}{\pi} \tag{2}$$

Therefore, from Eqs. 1 and 2

$$B_{af} = \frac{T_e \, T_t \, K_\theta \, a_f \, E_s}{\pi} \tag{3}$$

and

$$E_{af} = B_{af} \, \omega \tag{4}$$

where

$$\omega = \frac{\pi}{4 \, N^2} \tag{5}$$

where

$$N = \frac{\text{f.l.}}{D_o} \tag{6}$$

Therefore, from Eqs. 3, 4, and 5,

$$E_{af} = \frac{T_e \, T_t \, K_\theta \, a_f \, E_s}{4 \, N^2} \tag{7}$$

Since the beacon size will be less than the resolution limit of the detection instruments, it can be considered as a point source having an image which is a diffraction pattern, 84 percent of the energy falling into the Airy or first-diffraction disc. The illuminance of the image from a point source, E_{ab}, is then related to the incident illuminance, E_{ob}, the objective diameter, D_o, focal length, f.l., the transmittance loss, T_t, and the integrated resolution limit, β, by

$$E_{ab} = 0.84\ T_t\ E_{ob} \left[\frac{D_o}{\beta\ f.l.}\right]^{-2} \tag{8}$$

Note that the angle, β, approaches $[1.22\ \lambda/D_o]$ for perfect seing where λ is the light wavelength. E_{ob} is related to the beacon apparent solid angular subtend, Ω_b, the solar solid angular subtend at the beacon, Ω_s, and the beacon illuminance, E_b, and the atmospheric transmittance, T_e, so that

$$E_{ob} = T_e \frac{\Omega_b}{\Omega_s} E_b \tag{9}$$

but the beacon illuminance is directly related to the incident solar illuminance, E_s, and beacon reflectance, r_b:

$$E_{ob} = E_s\ r_b \tag{10}$$

and the beacon angular subtend is related to the projected beacon area, $a \cos\theta/2$ (i.e., the beacon mirror must be perpendicular to the bisector of the phase angle to be seen) and the range, R, so that:

$$\Omega_b = \frac{a \cos\frac{\theta}{2}}{R^2} \tag{11}$$

Combining Eqs. 6, 8, 9, 10, and 11

$$E_{ab} = \frac{0.84\ T_e\ T_t\ a \cos\frac{\theta}{2}\ E_s\ r_b}{\Omega_s\ R^2\ \beta^2\ N^2} \tag{12}$$

The apparent field and beacon illuminances are related to the photographic contrast for detection, C_p, by the term

$$C_p = \frac{E_{ab} - E_{af}}{E_{af}} = \frac{E_{ab}}{E_{af}} - 1 \tag{13}$$

By direct substitution of Eqs. 7 and 12 into Eq. 13

$$C_p + 1 = \frac{3.36\ a \cos\frac{\theta}{2}\ r_b}{K_\theta\ a_f\ \Omega_s\ \beta^2\ R^2} \tag{14}$$

Transposing

$$\frac{a r_b}{(C_p + 1)} = \frac{K_\theta\ a_f\ \Omega_s\ R^2\ \beta^2}{3.36 \cos\frac{\theta}{2}} \tag{15}$$

Note that this relationship is independent of the solar illuminance, transmittance values, and f/number (N), except as they affect the contrast and resolution values, of the system. In cases where seeing conditions govern the resolution angle, β, the camera diameter will only affect the film speed used and the time over which seeing conditions are integrated.

A log-log plot of the area factor, $ar_b/(C_p + 1)$, versus β yields a series of straight lines for each phase angle. The visual and photographic beacon areas are both closely related. Figures 1 and 2 are plots for ranges of 400 nautical miles and 207,000 nautical miles, earth-moon mean distance, respectively.

Let us now compare visual telescope theory with the above.

3. VISUAL TELESCOPE PHOTOMETRY THEORY

The apparent field brightness of a telescope can be reduced if the exit pupil, d, is smaller than the eye pupil, d_e, which is the case for astronomical telescopes, by the ratio of their areas, $(d/d_e)^2$ so that

$$B_{af} = T_e\ T_t \left(\frac{d}{d_e}\right)^2 B_f \tag{16}$$

which is the same as Eq. 1 when $d = d_e$

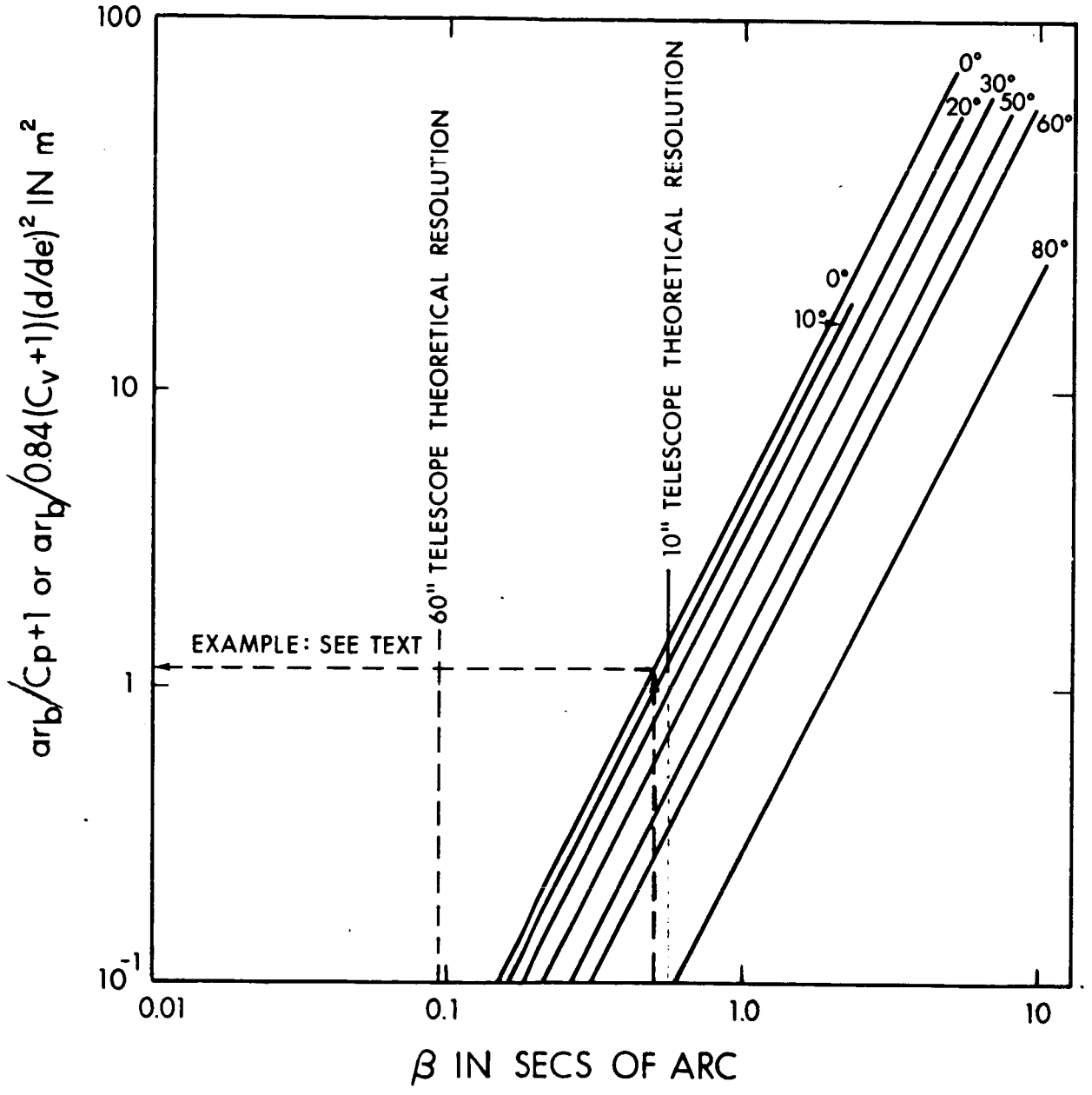

FIG. 1 AREA FACTOR VS RESOLUTION LIMIT FOR VARIOUS PHASE ANGLES FOR 0° LONGITUDE AT A 207,000 NAUTICAL MILE RANGE

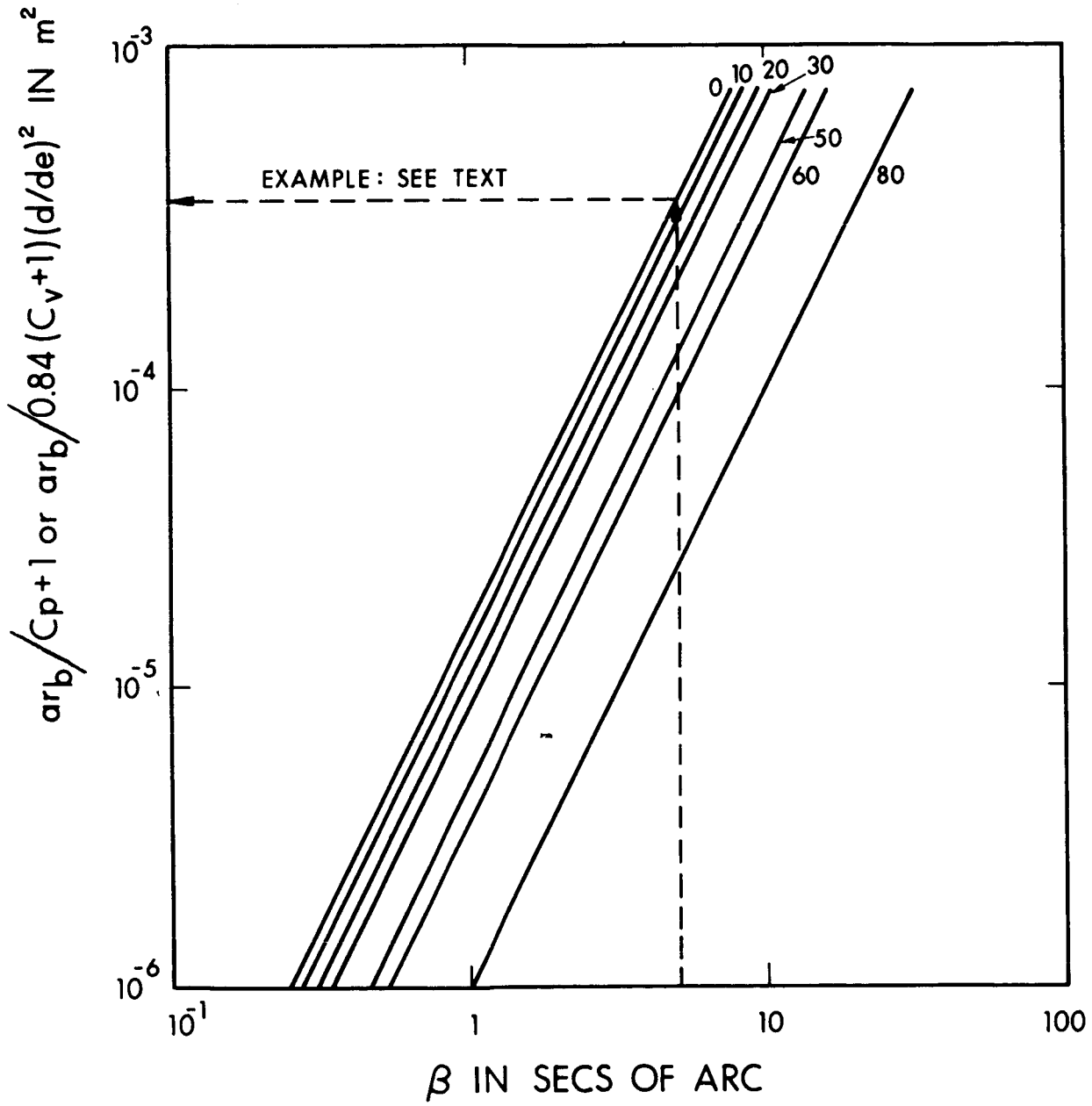

FIG. 2 AREA FACTOR VS RESOLUTION LIMIT FOR VARIOUS PHASE ANGLES FOR 0° LONGITUDE AT 400 NAUTICAL MILES

By combining Eqs. 2 and 16

$$B_{af} = T_e\, T_t \left(\frac{d}{d_e}\right)^2 \frac{K_\theta\, a_f\, E_s}{\pi} \tag{17}$$

The apparent brightness of the beacon, B_{ab}, and the apparent illuminance are related to the solid angle subtended by the eye, ω_e, after magnification, M, of the angle resolved, β, by

$$B_{ab} = \frac{E_{ab}}{\omega_e} \tag{18}$$

$$= \frac{E_{ab}}{\frac{\pi}{4}(\beta M)^2} \tag{19}$$

Now E_{ab} is related to the incident illuminance, E_{ob}, and the magnification and transmittance by

$$E_{ab} = T_t\, E_{ob}\, M^2 \tag{20}$$

By substituting Eqs. 9, 10, 11, and 20 into Eq. 19

$$B_{ab} = \frac{T_t\, T_e\, E_s\, r_b\, a \cos\frac{\theta}{2}}{\frac{\pi}{4}\Omega_s\, \beta^2\, R^2} \tag{21}$$

Now the visual contrast, C_v, required for beacon reflection is related to B_{ab} and B_{af} by

$$C_v = \frac{B_{ab} - B_{af}}{B_{af}} = \frac{B_{ab}}{B_{af}} - 1 \tag{22}$$

Therefore, combining Eqs. 17, 21, and 22 yields

$$C_v + 1 = \frac{4\, a \cos\frac{\theta}{2}\, r_b\, d_e^2}{K_\theta\, a_f\, \Omega_s\, d^2\, \beta^2\, R^2} \tag{23}$$

Recombining and setting 4 = [3.36/0.84]

$$\frac{a r_b}{0.84\,(C_v + 1)} \left[\frac{d_e}{d}\right]^2 = \frac{K_\theta\, a_f\, \Omega_s\, R^2\, \beta^2}{3.36 \cos\frac{\theta}{2}} \tag{24}$$

Note that the right side of the equation is the same as Eq. 15 and that the left side differs only by the substitution of C_v for C_p and the field brightness reduction ratio of $(d/d_e)^2$ and the fact that eye contrast values already integrate the 0.84 Airy disc energy collection factor. Therefore, with the substitution of the left side of Eq. 24 for the left side of Eq. 15, Figs. 1 and 2 can be used for both photographic and visual beacon calculations. Note that Eq. 24 is independent of the solar illuminance, transmittance, and telescope diameter values except as they affect the contrast and resolution values of the detection system.

The exit pupil, d, is a function of the telescope objective diameter and magnification so that

$$d = \frac{D_o}{M} \tag{25}$$

Equation 24 then becomes

$$\frac{a r_b\, d_e^2}{0.84\,(C_v + 1)} \left[\frac{M}{D_o}\right]^2 = \frac{K_\theta\, a_f\, \Omega_s\, R^2\, \beta^2}{3.36 \cos\frac{\theta}{2}} \tag{26}$$

where M/D_o is the magnification per unit diameter.

Now let us analyze Eqs. 15 and 16 before discussing C_p and C_v in depth. For any given phase angle and landing site, the terms $K_\theta\ a_f\ \Omega_s/3.36$ are constant. Both K_θ and a_f are discussed in another section. Therefore, the beacon area varies as the square of the range and the square of the resolution angle. For any given viewing case, the range will be constant. Therefore, the resolution angle chosen will be a major factor in determining beacon area. This choice is, therefore, the subject of a complete section. Looking at the left side of Eqs. 15 and 16, the area will be inversely proportional to the beacon reflectance. Of all the variables in each equation, this probably has the greatest possible range in values depending on the degradation analysis and space micrometeoroid data one uses. Therefore beacon reflectance is also the subject of a separate section.

Both equations have similar terms $(C_p + 1)$ and $C_v + 1)$ related to photographic and visual detection contrast respectively. It will be shown that both C_p and C_v are less than 1 so that the beacon areas required are relatively insensitive to contrast changes. The contrast values will be discussed in the next section.

Finally, the visual detection is highly dependent on the magnification per unit telescope diameter where in practice the ratio will be between 0.4 and 2.0 for most conditions. Since the practical magnification per unit telescope diameter seems inversely proportional to seeing conditions which limit β most of the time, using limited data by Bowen, then the area of the beacon appears to vary as β^4 which indicates the great dependence of beacon detection on seeing conditions.

4. CONTRAST

The degree of photographic or visual contrast required for detection is dependent on both the desired probability of detection and the detector efficiency.

4.1 Photographic contrast

Photographic contrast used herein is given by

$$C_p = \frac{E_{ab} - E_{af}}{E_{af}} = \frac{E_{ab}}{E_{af}} - 1$$

Films are classified in terms of development contrast, γ, density differences, ΔD, where D = log 1/transmission, and Δ log I, the differences in the logs of the exposures in meter-candle-seconds, so that

$$\gamma = \frac{\Delta D}{\Delta \log I} \tag{27}$$

but

$$I = Et \tag{28}$$

so that

$$\gamma = \frac{\Delta D}{\Delta \log Et} = \frac{\Delta D}{\log E_{ab}\, t - \log E_{af}\, t} = \frac{\Delta D}{\log \frac{E_{ab}}{E_{af}}} \tag{29}$$

For each photographic film there is an rms graininess density variation of standard deviation, σ, where σ is measured in the same units as D. For a detection probability of 99.7 percent, a density difference ΔD

of 3σ is required. γ is the slope of the D versus log I curve measured at field brightness exposure energy, I_f, level. σ is measured from microdensitometer readings and will vary according to the slit width, d, of the microdensitometer, which ranges from 5 to 25 microns (0.0002 to 0.001 inch) wide according to the relationship

$$\sigma \cdot d = k \tag{30}$$

Therefore, the microdensitometer used to evaluate lunar photographs should have the same width as the slit used in the rms graininess measurement, to achieve the results predicted from theory.

For minimum seeing disturbances, the film exposure time should be short and, therefore, the exposure index high. Exposures, t, 1/25 second or less are desirable. The exposure energy, I, is given by the following term derived by combining Eqs. 7 and 28:

$$I = \frac{T_e\, T_t\, K_\theta\, a_f\, E_s\, t}{4N^2} \tag{31}$$

and

$$\text{A.S.A. film reading} = \frac{1}{I} \tag{32}$$

For $T_e = 0.70$, $T_f = 0.70$, $K_\theta = 1$, $a_f = 0.065$, $E_s = 140{,}000$ lumens/m^2
$N = 16$, and $t = 0.04$

$$\text{A.S.A.} = \frac{1}{0.174} = 5.75$$

For films of equal or higher A.S.A. value, many have γ's equal or greater than 3.0 and σ's less than or equal to 0.1. Therefore

$$C_p + 1 = \log^{-1} \frac{0.1}{3.0} = 1.08 \qquad \text{(by combining Eqs. 13 and 29)}$$

This value has been used in all photographic calculations and appears quite conservative due to the conservative film assumptions.

Assume that 1/2 sec seeing, β = 1/2 sec, is practical for a given site, i.e., at least 10 percent of the time at Pic-du-Mich in France and that the telescope has a resolution better than 1/2 sec of arc. Then from Fig. 1 drawn with this example the area factor $ar_b/(C_p + 1)$ is 1.13 square meters for a 0-degree phase angle sighting at 0 degree longitude. Therefore, for a reflectance of 0.80 and $(C_p + 1)$ = 1.08 above, a = 1.53 square meters (16.5 square feet).

Other photographic detection beacon areas were calculated in a similar fashion.

4.2 Visual Contrast

Visual contrast required for detection has been the subject of numerous investigations, many of which are summarized by Taylor (1964). In general, most calculations refer to the work of Blackwell (1946) who reported the Tiffany Data. These data represented special viewing conditions characterized by the following factors:

1. Uniform circular targets
2. Uniform background
3. Binocular vision
4. Known time of stimulus
5. Known direction of stimulus
6. Trained observers

The Tiffany data are reported for a 50-percent probability of detection, C_{50}. Taylor has summarized various correction factors for modifying the original Blackwell data for application to practical conditions. These are summarized in Table 1. For beacon calculations, the contrast, C_v, used is related to the correction values in the table, K_p, K_b, K_v, K_t, and the original data, Tiffany Data C_{50}, by

$$C_v = K_p K_b K_v K_t C_{50} \qquad (33)$$

TABLE 1

CORRECTION FACTORS FOR BLACKWELL DATA

					Factor
1.	1. Detection Probability, K_p				
	50%				1.0
	90%				1.50
	95%				1.64
	99%				1.91
	2. Target Properties, K_b				
		Known Factors			
	Location	Time	Size	Duration	
	X	X	X	X	1.00
	X		X	X	1.40
	X		X		1.60
	X			X	1.50
	X				1.45
		X	X	X	1.31
	3. Vigilance, K_v				1.19
	4. Training, K_t				
	Trained				1.00
	Untrained				1.90

Values of $K_p = 1.91$, $K_b = 1.40$, $K_v = 1.19$, and $K_t = 1.00$ were chosen representing a 99-percent detection probability, unknown flash time (i.e., not an omnidirectional beacon), a vigilant and trained observer or $C_v = 3.18\ C_{50}$. This is the range of presently accepted conversion factors for the Tiffany data. Even if this factor is in error by a factor of 2, beacon areas will only increase by 20 percent for the worst practical telescopic visual case.

The visual contrast is a function of apparent field brightness, B_{af}, and apparent beacon angular subtend, $M\beta$. B_{af} can be determined from a plot of $B_{af}\ d_e^2$ versus B_{af} (Fig. 3) where by rearranging Eq. 16

$$B_{af}\ d_e^2 = T_e\ T_t\ d^2\ B_f \tag{34}$$

which by substitution of Eq. 25 is

$$B_{af}\ d_e^2 = T_e\ T_t \left[\frac{D_o}{M}\right]^2 \frac{K_\theta\ a_f\ E_s}{\pi} \tag{35}$$

For the 28X, 1.58-inch CM sextant sighting on 0-degree phase angle at $T_e = 1.0$, $T_t = 0.27$, $D_o/M = 1.443$ mm $= d$, $K_\theta = 1$, $a_f = 0.065$, $E_s = 14.0$ candles/cm^2. Therefore, $B_{af}\ d_e^2 = 1.61 \times 10^{-3}$ candles (and log $B_{af}\ d_e^2 = -3.206$).

Reading from Fig. 3, which is drawn showing this example, the apparent field brightness is 1.58×10^{-2} candles/cm^2.

Original smoothed Tiffany data, taken from Blackwell (1946) and converted to brightnesses in candles/cm^2, are shown in Fig. 4. Assuming a sextant resolution of 5 seconds, which is conservative compared with the 3.5 seconds value determined from $(1.22\ \lambda/D_o)$, the apparent beacon angular subtend will be 2.33 minutes of arc. A cross plot of C_v versus θ, not shown here, for constant, $B_{af} = 1.58 \times 10^{-2}$, using Fig. 4 for cross plot data, shows that $C_{50} = 4.95 \times 10^{-2}$ at $\theta = 2.33$ minutes. From above, $C_v = 3.18\ C_{50}$. $\therefore C_v + 1 = 1.157$. Knowing $B_{af}\ d_e^2$ and B_{af}

$$d_e = \sqrt{\frac{B_{af}\ d_e^2}{B_{af}}} \tag{36}$$

$= 3.2$ mm for the above case

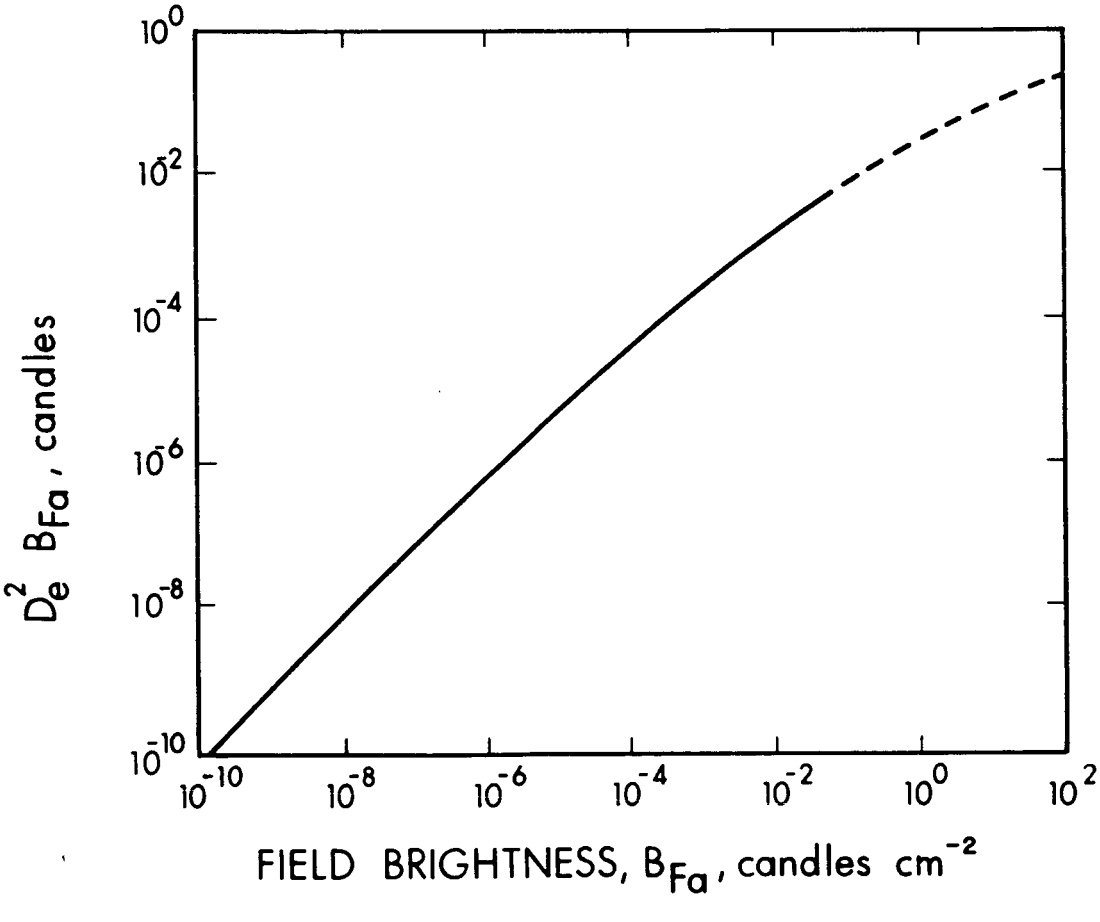

FIG. 3 RESPONSE OF THE PUPIL OF THE EYE TO FIELD BRIGHTNESS LEVEL

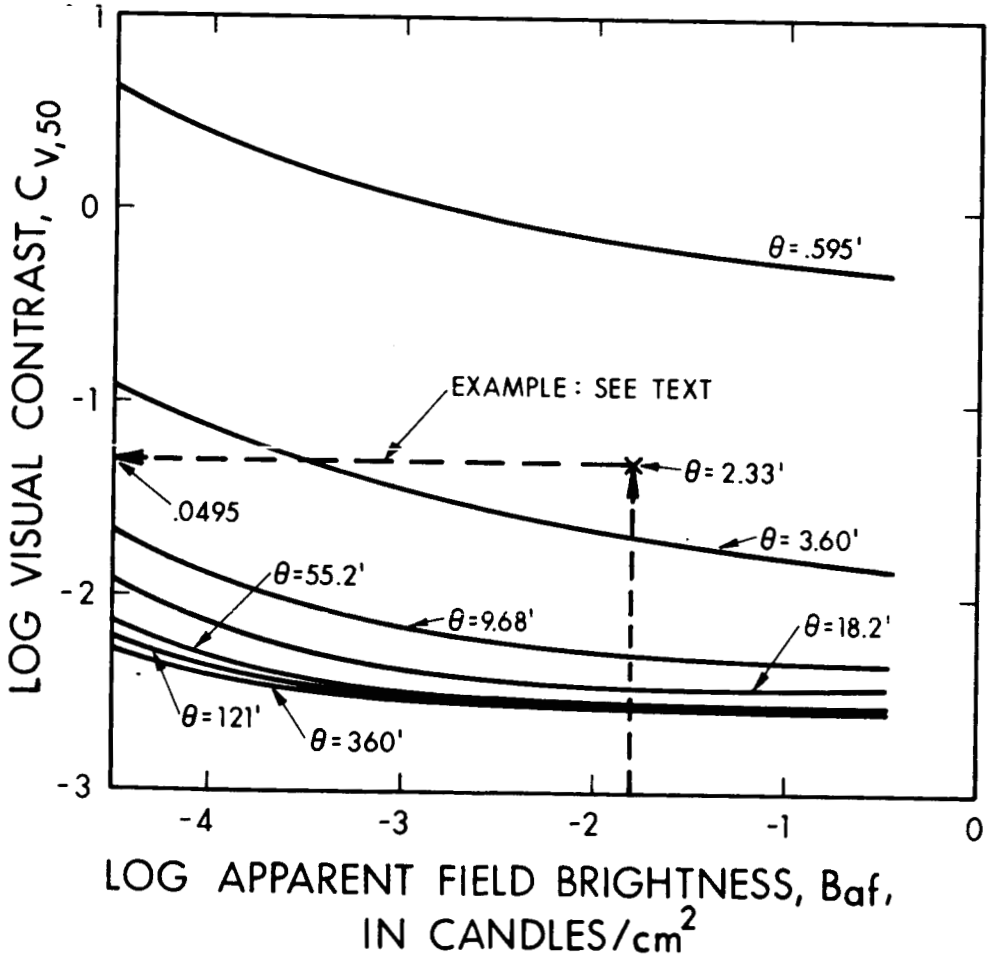

FIG. 4 VISUAL CONTRAST VS FIELD BRIGHTNESS FOR VARIOUS ANGULAR SUBTENDS, [illegible]

Assume $r_b = 0.80$; d was 1.443 mm from above. From Fig. 2 for a $\beta = 5$ seconds of arc resolution

$$\frac{ar_b}{0.84\ (C_v + 1)\left(\frac{d}{d_e}\right)^2} = 4.21 \times 10^{-4}\ m^2$$

Substitution of the values listed above yields a required beacon area of 1.03 cm^2 or 0.16 square inch. Other beacon areas for visual detection were calculated in a similar fashion. This corresponds to a spherical beacon diameter, d_s, of 4.95 meters (or 16.3 feet) disregarding the negative contrast effects of the apparently nonreflective portions of the moon. The spherical diameter is related to the area by the relationship

$$d_s = \frac{8}{\alpha}\sqrt{\frac{a}{\pi}} \qquad (37)$$

where α is the solar angular subtend.

5. BEACON REFLECTANCE

Possible degradation in the beacon reflectance is the major unknown in sizing the lunar beacon. Empirical and experimental analysis of the problem by Button (1964), Marks (1964), and others have predicted or extrapolated losses in spectral reflectance from between 1 and 50 percent due to uv, high energy proton, and micrometeorite impingement. No space experimental data are available to corroborate these analyses, though an experiment is now being planned to study the degradation of reflective samples in space.

Unprotected aluminum has a practical visible reflectance of 91 percent. Therefore, the assumed reflectance value of 0.80 percent would allow an 11-percent reflectance loss due to lunar dust, coating transmittance, micrometeorite damage, etc., and appears valid based on some reflectance predictions.

Silicon-monoxide-overcoated aluminum has a visible reflectance of 87 percent, when deposited under standard development conditions. Though this reflectance system is 4 percent lower than aluminum and although silicon monoxide coatings are more susceptible to failure when folded over sharp corners as in an inflatable beacon, aluminum coatings overcoated with a 1000Å-micron-thick silicon monoxide coating show 1.2 times less degradation over comparable intensities of simulated micrometeorite flux. Silicon monoxide overcoatings have the added advantage that they are much more easily cleaned than aluminum alone. Quartz-overcoated aluminum will yield reflectance values of 88 percent over the visible spectrum and have high abrasion resistance also. However, quartz overcoatings are supplied by only a limited number of installations at this time.

Note that the reflectances cited are lower than textbook or experimental reflectance values. These lower values represent practical minimum limits for a metal mirror for this beacon program. Beacons with plastic substrates will have lower reflectance values.

6. SEEING CONDITIONS

For terrestrial telescopes, used either as photographic or visual instruments, the limiting angular resolution will determine to a large extent the detectability of a given beacon size. Since for most observatories the theoretical resolution of the telescope is achieved 10 percent or less of the night time, seeing is used in this analysis almost interchangeably with the integrated angular resolution of the detector instrument.

Seeing is a function of the changes in the index of refraction of the atmosphere through which the object rays pass to reach the telescope. Seeing is therefore an angular condition rather than a uniform loss of intensity which is a transmittance loss, or a non-uniform loss of intensity over the aperture called scintillation.

APPENDIX B

APPLICATION OF SUN-PUMPED LASER FOR LUNAR BEACON

A sun-pumped laser utilizes reflected photons from the sun to excite a Yttrium Aluminum Garnet (YAG) laser rod. Normally, lasers are excited by photons from a flash tube or an electrode discharge.

1. ADVANTAGES AND DISADVANTAGES

The use of a sun-pumped laser as the light source for a lunar beacon is attractive because of the power savings attendant with the direct utilization of solar energy. Additional advantages include the ease with which the output may be collimated and directed, using small optical components, and the ease with which it may be modulated. The principal problem in the use of a sun-pumped laser as a lunar beacon is providing adequate cooling for the laser material itself. The mechanics of tracking the sun with the laser's concentrator mirror and aiming the laser output to the earth are problems common to other lunar-solar tracking beacons using oriented solar cell panels to supply electrical power for other types of light sources.

The following subsections present some discussion of sun-pumped lasers and include data from recent EOS experiments. Suggestions are included for possible work to bring sun-pumped laser beacons closer to a flight hardware status.

2. CHOICE OF MATERIALS AND SOLAR CONCENTRATORS

The laser material chosen must have broad pump bands in the solar spectrum and as low a threshold as possible at temperatures in the vicinity of $300^{\circ}K$. A complete survey of laser materials that have been investigated was recently published by EOS (Ref. 1). Of all the materials, neodymium-doped YAG appears to be the best presently

available for use in sun-pumped laser beacons. The laser output from Nd^{3+}:YAG is at 1.06 microns. Continuous radiation has been obtained from small Nd^{3+}:YAG rods pumped with tungsten lamps with as little as 360 watts input power (Ref. 2).

The optimum concentrator configuration is not universally agreed upon. Paraboloidal concentrators give the highest attainable flux density (Ref. 3). However, with this design it is difficult to obtain efficient pumping of a laser rod since several passes of the rays through the rod are necessary to obtain adequate absorption at the pump bands.

One of the approaches successfully employed at EOS is to mount the laser rod along the axis of a paraboloidal mirror, near the focus, and use a conical lens surrounding the rod to produce a cylindrical image of the sun. Figure 1 is a photograph of such a configuration employed at EOS.

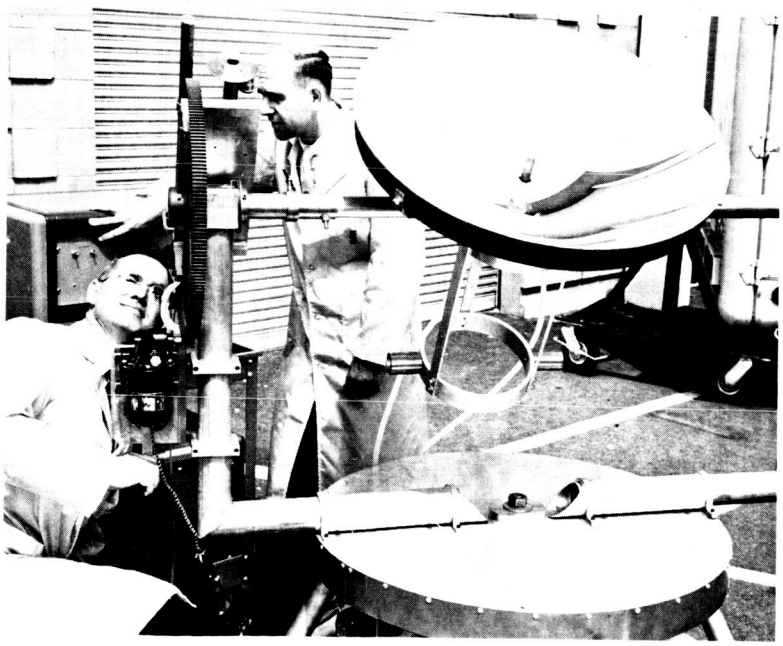

YAG-NEODYMIUM SUN-PUMPED LASER

In practice, the conical lens is filled with a liquid which serves to conduct heat from the laser rod. A special technique for processing a 3M fluorochemical FC-75 has been developed and has made it possible to utilize its excellent cooling characteristics in this application. It is possible that the cooling system could be designed so as to utilize the back side of the solar concentrator for radiative heat rejection, the coolant being circulated in tubes attached to the collector.

3. EOS EXPERIMENTS

The present EOS sun-pumped laser utilizes a 30-inch electroformed mirror to produce 45 milliwatts from a Nd^{3+}:YAG laser rod. The threshold has been observed to correspond to the radiation received on approximately half the mirror area. The 45-milliwatt output was obtained when the measured solar irradiance was 950 watts/cm^2 at the collector, which is about 40 percent less than the solar constant in space (1350 watts/m^2).

The principal areas, unique to sun-pumped laser beacons, where additional effort could be of most benefit are the following:

1. Improved solar concentrating systems
2. Improved laser materials
3. Design and development of cooling systems

EOS is currently engaged in a company-sponsored program to improve the optical system for collecting and concentrating the sun's energy on the laser rod. Hemispherical concentrators are being investigated and additional work should be devoted to other types of systems.

The second area is probably the most fruitful from the standpoint of increasing the laser output per unit beacon weight. The goal is to obtain a better match between the pumping spectrum and the absorption spectrum. The trivalent rare-earth crystal host lasers have very narrow and relatively weak 4f-4f parity-forbidden absorptions and so

exhibit inherently low system efficiencies when pumped with any of the high-energy broadband sources. Work is being done in the direction of energy transfer from a strong broadband absorber coexisting in the lattice structure to the rare-earth laser ion. Indications are that an immediate gain of 2 in efficiency (YAG:Nd^{3+}, cr^{3+}) is available and long-term gains of nearly an order of magnitude may be expected.

From the standpoint of bringing about a practical working beacon, the investigation of appropriate cooling systems is of extreme importance. If these engineering problems can be solved, the success of the sun-pumped laser beacon is assured.

REFERENCES

1. M. L. Bhaumik, L. W. Carrier, N. E. Johnson, "Characteristics of Lasers 1965," Laser Focus, Supplement, Data Publishing Co., P.O. Box 1, Newtonville, Mass.

2. Op. Cit., Table II

3. A. M. Zarem, D. D. Erway, Introduction to the Utilization of Solar Energy, McGraw-Hill Book Co., 1963

APPENDIX C

COMPUTATION OF TIME SPENT IN LIGHT CONE BY OBSERVER ON EARTH

$$K_1 = \sin\frac{\epsilon}{2} - \sin H_1 \ .$$

When, $K_1 < 0$, the reflected light is not visible from θ_1, ϕ_1;

When, $K_1 > 0$, the reflected light is visible from θ_1, ϕ_1;

When, $K_1 = 0$, the reflected light becomes visible, or just ceases to to be visible, from θ_1, ϕ_1 .

Here, θ_1, ϕ_1 are the longitude and latitude, respectively, of an observer on the earth. Also, $\epsilon/2$ = half angle of light cone ($\epsilon/2 \sim 16$ min. of arc), where

$$\frac{\epsilon}{2} = \frac{R_s}{R_{sm}}$$

Here, R_s = radius of sun = 6.965×10^5 km, R_{sm} = sun-moon distance, given by

$$R_{sm} = \left[\left(R_e \bar{X}_{em} + Au \bar{X}_{se}\right)^2 + \left(R_e Y_{em} + Au Y_{se}\right)^2 + \left(R_e Z_{em} + Au Z_{se}\right)^2\right]^{1/2}$$

where, $\bar{X}_{em}$, ---, Z_{se} are the normalized coordinates of the moon and earth, taken from the JPL ephemeris tapes, and R_e = radius of earth = 6378.3255 km, Au = astronomical unit = 149,599,000 km. The angle H_1 is the angle subtended at the reflector between the axis of the light cone and a line from the reflector to the point θ_1, ϕ_1 on the earth's surface. Here,

$$\sin H_1 = \frac{\left(V_1^2 + V_2^2 + V_3^2\right)^{1/2}}{Du Z_1}$$

where

$$V_1 = p_z(B - B_1) + p_y(C_1 - C) + \frac{BC_1 - B_1C}{D}$$

$$V_2 = p_z(A_1 - A) + p_x(C - C_1) + \frac{A_1C - AC_1}{D}$$

$$V_3 = p_y(A - A_1) + p_x(B_1 - B) + \frac{AB_1 - A_1B}{D}$$

$$u = \left[\left(p_x + \frac{A}{D}\right)^2 + \left(p_y + \frac{B}{D}\right)^2 + \left(p_z + \frac{C}{D}\right)^2\right]^{1/2}$$

$$Z_1 = \left[\left(p_x + \frac{A_1}{D}\right)^2 + \left(p_y + \frac{B_1}{D}\right)^2 + \left(p_z + \frac{C_1}{D}\right)^2\right]^{1/2}$$

The expressions for p_x, p_y, p_z are given on p. 9 of the proposal to MSC, and expressions for A, B, C and D are given on pp. 20-21 of the August monthly report. Finally,

$$A_1 = R_{elx}\, x_{11} + R_{ely}\, x_{12} + R_{elz}\, x_{13}$$

$$B_1 = R_{elx}\, x_{21} + R_{ely}\, x_{22} + R_{elz}\, x_{23}$$

$$C_1 = R_{elx}\, x_{31} + R_{ely}\, x_{32} + R_{elz}\, x_{33}$$

where

$$R_{elx} = -R_e \cos\phi_1 \cos(\theta_1 + \alpha_s + 15.0\, t)$$

$$R_{ely} = -R_e \cos\phi_1 \sin(\theta_1 + \alpha_s + 15.0\, t)$$

$$R_{elz} = R_e \sin\phi_1$$